UiT
THE ARCTIC
UNIVERSITY
OF NORWAY

Faculty of Science and Technology
Department of Chemistry

Advancing relativistic electronic structure methods for solids and in the time domain

—

Marius Kadek

A dissertation for the degree of Philosophiae Doctor – August 2018

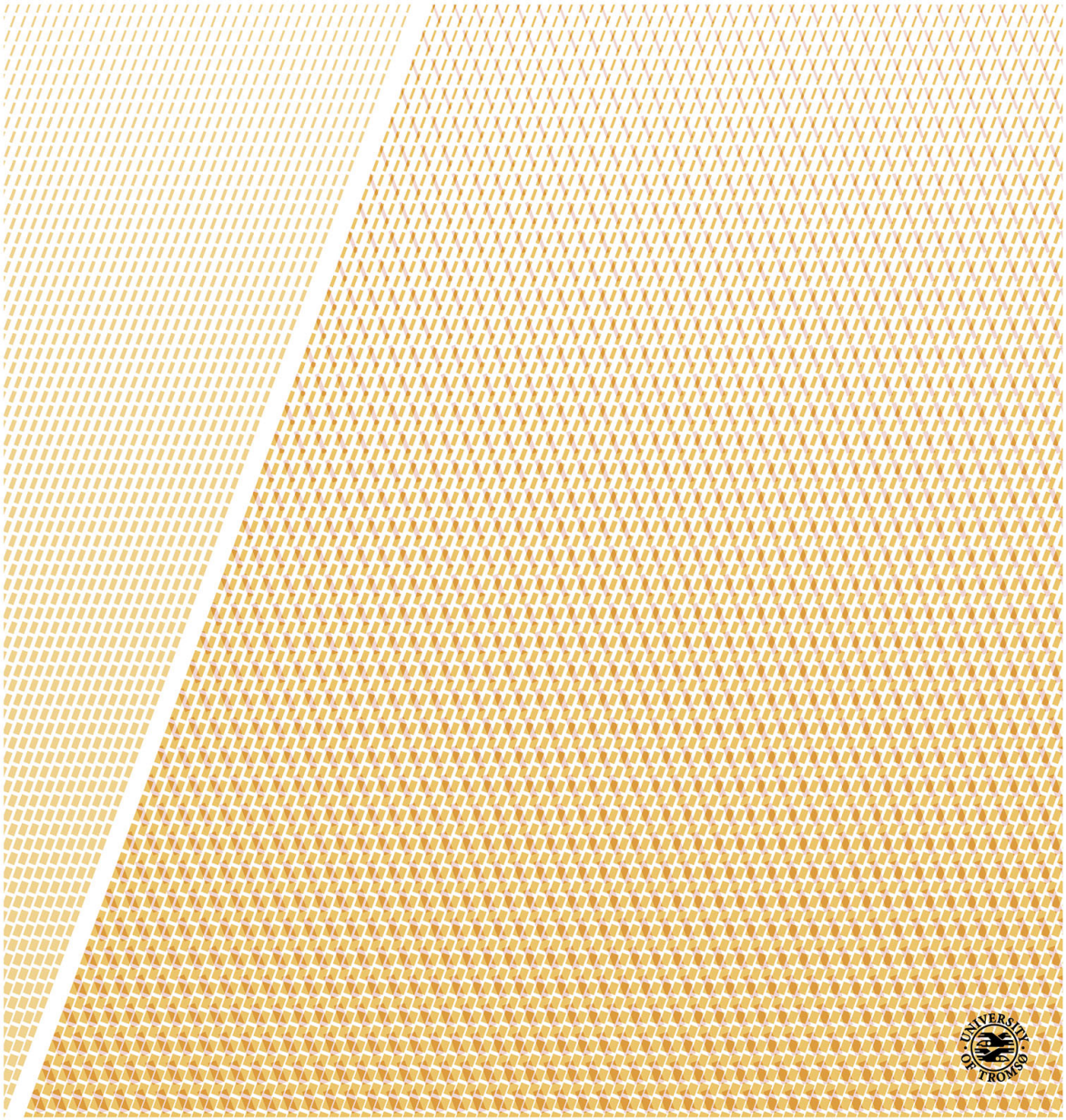

Abstract

Effects arising from the special theory of relativity significantly influence the electronic structure and properties of molecules and solid-state materials containing heavy elements. At the same time, the inclusion of the relativistic effects in theoretical and computational models increases their methodological complexity and the computational cost. In the solid state, additional challenges to the mathematical and algorithmic robustness of methods arise due to the infinite extent of the systems.

In this thesis, I present two extensions of quantum-chemical relativistic methods based on Gaussian-type basis functions in the study of the electronic ground-state of molecules: band-structure calculations of materials in the solid state, and simulations of the response of molecules that are subjected to an external time-dependent field by propagating their perturbed state in real time. The development of the relativistic methods for solids was preceded by an independent implementation of the theory at the non-relativistic level. In comparison to methods based on plane waves, the use of Gaussian-type basis functions in the solid-state community is limited. The relativistic method presented here is the first ever implementation of the Dirac-type equations using Gaussian-type basis functions for solid-state systems, and can be used to study one-, two-, and three-dimensional periodic systems on an equal footing for the entire periodic table. The time propagation method is a technically simpler alternative to perturbation approaches, and is applied here to probe relativistic effects on absorption and X-ray spectra, and nonlinear optical and chiroptical properties of molecules. Our work in the both areas provides a technology with the potential to predict properties of novel materials, and to support the interpretation of experiments.

Contents

List of Papers

This thesis is based on the following scientific publications.

I M. Repisky, L. Konecny, **M. Kadek**, S. Komorovsky, O. L. Malkin, V. G. Malkin and K. Ruud, "Excitation Energies from Real-Time Propagation of the Four-Component Dirac–Kohn–Sham Equation", *J. Chem. Theory Comput.* **11** (2015), 980–991.

II **M. Kadek**, L. Konecny, G. Bin, M. Repisky and K. Ruud, "X-ray absorption resonances near $L_{2,3}$-edges from real-time propagation of the Dirac–Kohn–Sham density matrix", *Phys. Chem. Chem. Phys.* **17** (2015), 22566–22570.

III L. Konecny, **M. Kadek**, S. Komorovsky, O. L. Malkina, K. Ruud and M. Repisky, "Acceleration of Relativistic Electron Dynamics by Means of X2C Transformation: Application to the Calculation of Nonlinear Optical Properties", *J. Chem. Theory Comput.* **12** (2016), 5823–5833.

IV L. Konecny, **M. Kadek**, S. Komorovsky, K. Ruud and M. Repisky, "Resolution-of-identity accelerated relativistic two- and four-component electron dynamics approach to chiroptical spectroscopies", *J. Chem. Theory Comput.*, (submitted).

V **M. Kadek**, M. Repisky and K. Ruud, "All-electron fully relativistic Kohn–Sham theory for solids based on the Dirac–Coulomb Hamiltonian and Gaussian-type functions", (in preparation).

Acknowledgements

The acknowledgement section is included in all books and theses, so one might get an impression that it is a common courtesy to thank people for their support. This could not be further away from truth. Expressing gratitude to people that are in some way connected to the author's struggle during a PhD project or writing stages is so much more than just a "common courtesy". I truly learned about how invaluable the support of the people mentioned here is during the many dark and stormy phases of my PhD project, and writing "thank you" here now seems to be the least I can do for them. So thank you, for being there, when I needed it.

Now let me be more specific. First of all, I thank my supervisor Kenneth Ruud and my co-supervisor Michal Repisky, for providing interesting projects that kept me occupied, and for introducing me to the relativistic world and the ReSpect program. Next, I would like to thank my coworker and friend Lukas Konecny, for sharing some parts of this journey together with me, and for countless discussions on an unlimited variety of topics. I thank Stanislav Komorovsky for scientific debates on multiple projects, and for introducing me to board games. It was fun, despite the fact that you always won.

I express my thanks to all co-authors and contributors, the ones that have not been mentioned yet are Bin Gao, Vladimir Malkin, and Olga Malkin. I thank the HPC staff for taking care of the supercomputer Stallo, and I thank the supercomputer for running my calculations day and night, and usually not complaining a lot about it. I am grateful for the fantastic working environment provided by the Hylleraas Centre for Quantum Molecular Sciences, the former Centre for Theoretical and Computational Chemistry (CTCC), and the Department of Chemistry, and I thank my colleagues and friends, Maarten, Roberto, Magnus, Radovan, Karen, Magnar, and Karolina.

Finally, I cannot describe with words how grateful I am to my parents and to my brother, Marek. My PhD journey would not have been possible without your constant support and love. Special thanks goes to the people at the Department of Theoretical Physics at Comenius University, for providing me with high-quality education, some of which I still get to apply on a daily basis.

Abbreviations

The following abbreviations are all defined in the text. This list is to allow for easy reference.

1c	1-component
2c	2-component
4c	4-component
DFT	density functional theory
DHF	Dirac–Hartree–Fock
DKS	Dirac–Kohn–Sham
DOS	density of states
ECD	electronic circular dichroism
GGA	generalized gradient approximation
GHF	general Hartree–Fock
GTO	Gaussian-type orbital
HF	Hartree–Fock
KS	Kohn–Sham
LDA	local density approximation
LvN	Liouville–von Neumann
MO	molecular orbital
ORD	optical rotatory dispersion
QED	quantum electrodynamics
RHF	restricted Hartree–Fock
RKB	restricted kinetic balance
SCF	self-consistent field
SOC	spin–orbit coupling
TDSCF	time-dependent self-consistent field
TR	time reversal
UHF	unrestricted Hartree–Fock
X2C	exact 2-component
XC	exchange–correlation

Notations and conventions

Here I summarize basic conventions and notations used throughout this thesis.

Unless otherwise stated, Hartree atomic units are employed:

$$\hbar = e = m_\mathrm{e} = \frac{1}{4\pi\varepsilon_0} = 1,$$

where $\hbar$ is the reduced Planck constant, e is the elementary charge, m_e is the electron mass, and ε_0 is the vacuum permittivity. We use the following derived units:

$$E_\mathrm{h} = \frac{m_\mathrm{e} e^4}{(4\pi\varepsilon_0\hbar)^2}, \qquad\qquad a_0 = \frac{4\pi\varepsilon_0\hbar^2}{m_\mathrm{e} e^2},$$

where a_0 is the Bohr radius, and E_h is the Hartree energy. The speed of light in atomic units is

$$c = 137.035\,999\,074\, a_0 E_\mathrm{h} \hbar^{-1}.$$

Some conventions:

- Operators are *not* denoted with a hat, and vectors and matrices are *not* typeset in bold (except three-dimensional vectors).
- 2-component Pauli-type wave functions and 4-component Dirac-type wave functions are referred to as *spinors* and *bispinors*, respectively.
- Square brackets denote vectors and matrices acting in the space of Kramers pairs, whereas matrices acting in the space generated by the large and small components of the basis are typeset with round brackets.
- Integration over $\mathbb{R}^3$ is assumed, whenever the integration domain is not denoted explicitly, *i.e.* $\int \ldots \equiv \int_{\mathbb{R}^3} \ldots$.
- The most important equations are typeset in a frame.

Common notation:

iff	if and only if, equivalence
x^μ	four-vector coordinates
$\boldsymbol{r}, \boldsymbol{x}, \boldsymbol{y}$	3-dimensional vectors
$\boldsymbol{m}, \boldsymbol{m}', \boldsymbol{n}$	3-dimensional lattice vectors
$\mathbb{R}, \mathbb{C}, \mathbb{Z}$	real numbers, complex numbers, integers
$\sum_a u^a v_a \equiv u^a v_a$	Einstein summation convention
$\chi_a(\boldsymbol{r}), \chi_b(\boldsymbol{r}) \in \mathbb{C}^{4\times 1}$	basis bispinors
$\chi_\mu(\boldsymbol{r}), \chi_\nu(\boldsymbol{r}) \in \mathbb{C}^{4\times 4}$	matrix of basis functions
$\varphi_p(\boldsymbol{r}), \varphi_q(\boldsymbol{r}) \in \mathbb{C}^{4\times 1}$	4-component SCF solutions
$\delta(\boldsymbol{r})$	3-dimensional Dirac delta function
δ_{ij}	Kronecker delta (= Kronecker symbol)
ε_{ijk}	Levi-Civita symbol
0_n	zero $n \times n$ matrix
$\mathbb{I}_n$	$= \mathrm{diag}(1 \ldots 1)$, $n \times n$ identity matrix
$A \otimes B$	tensor product of matrices A and B
$\boldsymbol{\sigma} \equiv (\sigma_x, \sigma_y, \sigma_z)$	vector of Pauli matrices
$f(x) \sim g(x) \quad (\mathrm{as}\, x \to x_0)$	$\lim_{x\to x_0} f(x)/g(x) = 1$
$^*, ^\dagger$	complex and Hermitian conjugation
$\langle A \rangle \equiv \langle A \rangle_\psi \equiv \langle \psi \vert A \vert \psi \rangle$	expectation value of an operator A
$[A, B]$	$= AB - BA$, commutator
$\{A, B\}$	$= AB + BA$, anti-commutator
$\mathrm{Tr}\, A$	trace of A

Introduction

> What I cannot create, I do not understand. Know how to solve every problem that has been solved.
>
> *Richard Feynman*

> Scientific progress happens in two ways, either driven by new ideas or by new tools. The first half of the twentieth century was the time of new ideas, the second half was the time of new tools. New ideas are more exciting but new tools are often more important. For the twenty-first century, it seems that the most important contribution of physicists is to build new tools for other sciences.
>
> *Freeman Dyson*

The 20th century gave rise to two fundamental physical theories that changed our understanding of the world. Einstein's *theory of relativity*[1] enabled us to comprehend the relationship between space and time, resolved the inconsistency of Newtonian mechanics with Maxwell's equations of electromagnetism, and eventually lead to the geometric theory of gravitation. *Quantum theory* described matter at the microscopical level, and lead to the unified theory of the electromagnetic, weak, and strong interactions (the Standard Model). Applications of quantum mechanics affect our everyday lives, and range from laser and semiconductor (transistors and light-emitting diodes) technologies to magnetic resonance imaging used in medicine. Quantum mechanics also explains the chemical bond,[2] which plays an important role in molecules, including large biological complexes. Quantum chemistry, quantum computing, condensed matter physics, and

quantum optics are some of several fields of science that apply quantum theory to various domains.

The original quantum mechanics, governed by the Schrödinger equation,[3] is incompatible with the laws of the theory of relativity, and does not account for relativistic effects, *i.e.* effects arising from the finite speed of light. This problem was solved by Dirac in 1928 who formulated the relativistic counterpart of the Schrödinger equation for the electron, known as the Dirac equation.[4] It was quickly realized from studies of X-ray spectroscopy of heavy elements that relativity affects electrons close to the nuclei,[5] but the influence of relativity was later observed on valence states as well.[6]

The importance of including relativistic effects in theoretical models of molecules and solids containing heavy elements is well established today. For instance, relativity explains the chemical differences between gold and silver,[7–9] including the yellow color of gold,[10] why mercury is in its liquid state at room temperature,[11,12] and why lead-acid batteries commonly used in cars work while tin-acid batteries do not work.[13] Relativistic effects cause significant structural changes in stable phases of solids,[14–17] and can alter the electronic ground state from metallic to insulating.[18] Topological insulators,[19–21] spintronics,[22–24] and various two-dimensional systems such as transition-metal dichalcogenides[25–27] and graphene-like honeycomb structures[28–31] have recently been of particular interest in solid-state research. Proper modeling of the fascinating properties of these systems requires that the coupling between the electron's spin and its angular momentum is taken into account; this so-called spin–orbit coupling naturally arises from the Dirac equation.

The role of computer simulations in aiding both theory and experiment has been increasing with the ever-growing power of computers and robustness of the computational methods. Determining many properties of realistic molecules and materials requires solving very complicated quantum mechanical equations. In principle, all information about an electronic state of a system is encoded in the many-electron wave function. However, solving the Schrödinger equation to obtain this wave function for large molecules and solids is an impossible task – we are cursed by an unfavorable scaling feature of the many-electron Schrödinger equation. Hence, a sequence of sophisticated approximations and simplifications that make the problem

manageable must be introduced. One of the goals of theoretical physicists and chemists is to develop techniques for feasible computer simulations of a wide range of phenomena of complex systems. These techniques must at the same time retain the ability to capture the elements of the theory that are essential for a proper description of the studied phenomena.

The objective of this doctoral thesis has been to advance the relativistic methods that are used to study the electronic structure and properties of molecules containing heavy elements to two distinct areas. The primary focus of this work has been the extension of the relativistic procedure that obtains the electronic ground state of molecules to treat systems in the solid state. The secondary task has been to subject molecules to a time-dependent external field, and propagate the perturbed electronic state in real time to probe various spectroscopic properties of the molecules. The relativistic effects have served as a uniting theme for these two objectives – the relativistic methods that account for the complex multi-component structure of wave functions are not as developed as their nonrelativistic counterparts. This fact is even more pronounced in the solid-state realm, where the infinite nature of the systems demands careful handling of both the mathematical and the algorithmic aspects of the method. The goal of this work has been to provide a technology and a tool that has the potential to predict properties of novel materials, aiding experiment as well as theoretical understanding. All methods developed as part of this work were implemented in the relativistic ReSpect program package,[32] and have used the vectorized integral library InteRest,[33] and exchange–correlation contributions have been evaluated using the XCFun library.[34]

This thesis is composed of five scientific articles referred to as **Paper I**–**V** in the text, and four introductory chapters. The first four papers deal with the real-time propagation method: we first introduced the method to the relativistic domain in **Paper I**, where we describe the details and the implementation of the approach; in **Paper II** we applied the propagation method to study the $L_2, 3$-edge X-ray spectroscopy; the method is further enhanced in **Paper III** and **IV** to allow for relativistic treatment of large molecules, and we study nonlinear optical properties (**Paper III**) and chiroptical properties (**Paper IV**) of molecules. Finally, **Paper V** is a manuscript, where we for the first time establish the relativistic method for band structure calculations of solid-state (periodic) systems based on

the Dirac-type equations and Gaussian-type orbitals. In the manuscript, we discuss this approach in great detail.

The aim of the four chapters in this thesis is to provide the necessary background to the scientific papers, and to introduce the basic principles used throughout the various topics that are discussed there. The purpose of this introductory text is more pedagogical than scientific, and the text is addressed to a reader interested in entering some of the fields addressed here. The detailed scientific introduction to each of the mentioned topics can be found in the individual papers. The reader is assumed to have some basic knowledge of a finished master student in physics or chemistry. This includes comprehension of fundamental concepts of quantum theory, linear algebra, multivariable calculus, and the Hartree–Fock method; some expertise in the Lagrangian and Hamiltonian mechanics, electromagnetism, and occupation number representation (second quantization) is needed only briefly in some sections.

The chapters are structured as follows. In Chapter 1, Dirac's relativistic one-electron quantum mechanics[4] is formulated and adapted to finite basis calculations.[35] Furthermore, time-reversal symmetry is discussed in the context of the relativistic framework. Chapter 2 summarizes the foundations of the Hartree–Fock and Kohn–Sham self-consistent field theories in the language of the one-electron density matrix.[36] The framework developed in these two chapters is then applied in Chapter 3 to the time domain, and in Chapter 4 to the solid-state systems. Chapter 3 contains a description of the method based on solving the Liouville–von Neumann equation by propagating the density matrix in real time. Our scientific contributions in **Paper I**–**IV** are summarized at the end of Chapter 3. Chapter 4 introduces the underlying elements of the band structure theory, and summarizes the contributions in **Paper V**, while showing some of the necessary modifications to the self-consistent method described in Chapter 2.

Chapter 1

Relativistic quantum theory

> There is nothing more practical than a good theory.
>
> *Kurt Lewin*

In this chapter I outline the Dirac's relativistic quantum theory of the electron,[4] and provide a language and basic concepts of the relativistic quantum mechanics that are employed throughout this thesis to study properties of molecules and solids. Needless to say, the chapter serves merely as an introduction to this rich topic, and I refer the interested reader to the textbooks of Dyall and Faegri,[37] Reiher and Wolf,[38] and the review article of Saue[39] for further reading.

Historically, relativistic quantum mechanics is a predecessor to quantum electrodynamics (QED), which is the fundamental fully Lorentz invariant quantum theory of interacting electrons, positrons, and photons. When considering a low-energy scale that is of interest in the areas of solid-state physics and chemistry, QED treatment of particles can safely be neglected for all except the heaviest elements of the periodic table, or in cases where very high accuracy of results is desired. However, relativity cannot be neglected entirely, as we discussed in the Introduction.

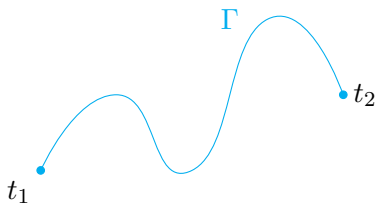

Figure 1.1. A curve depicting motion of a relativistic particle in 4-dimensional Minkowski spacetime.

1.1 The Dirac equation

1.1.1 Relativistic Hamiltonian

One way to derive the one-electron Dirac equation is to formulate the relativistic Hamiltonian which is then quantized in the spirit of Dirac's original work. Consider a particle moving along a curve Γ in 4-dimensional Minkowski space with the metric tensor $\eta = \mathrm{diag}(1, -1, -1, -1)$ (see Fig. 1.1). In absence of external fields the action integral S can be written as an integral of Lorentz-invariant infinitesimal spacetime intervals ds over the curve Γ, *i.e.*

$$S = k \int_\Gamma \sqrt{ds^2}, \tag{1.1}$$

where k is a dimensionality constant. Let x^μ denote coordinates in Minkowski space for $\mu = 0, 1, 2, 3$; and $x^0 \equiv ct$, where c is the speed of light and t denotes time. Using time t to parameterize Γ as $x^\mu \equiv x^\mu(t)$, we obtain

$$S = k \int_{t_1}^{t_2} \sqrt{\eta_{\mu\nu} \dot{x}^\mu \dot{x}^\nu}\, dt, \tag{1.2}$$

because $ds^2 = \eta_{\mu\nu} dx^\mu dx^\nu$ and $dx^\mu \equiv \dot{x}^\mu dt$ (the dot denotes the time derivative, and Einstein summation convention is implied). Expanding the sum over μ and ν gives

$$S = kc \int_{t_1}^{t_2} \sqrt{1 - \frac{v^2}{c^2}}\, dt, \tag{1.3}$$

where $v^2 \equiv \boldsymbol{v}^2 = \left(\dot{x}^1\right)^2 + \left(\dot{x}^2\right)^2 + \left(\dot{x}^3\right)^2$ is the particle's speed. We identify the Lagrangian as the integrand

$$L(\boldsymbol{x}, \boldsymbol{v}) = kc \sqrt{1 - \frac{v^2}{c^2}}. \tag{1.4}$$

The dimensionality constant k is determined by expanding the square root for $v \ll c$, and requiring that in the limit of $c \to \infty$ the Lagrangian coincides with the nonrelativistic kinetic energy (up to an additive constant). Then one finds that $k = -mc$, where m is the particle's rest mass. Hence

$$L(\boldsymbol{x}, \boldsymbol{v}) = -mc^2\sqrt{1 - \frac{v^2}{c^2}}. \tag{1.5}$$

To obtain the Hamiltonian $H = \boldsymbol{v} \cdot \boldsymbol{p} - L$, we evaluate the particle's momentum $\boldsymbol{p}$:

$$\boldsymbol{p} \equiv \frac{\partial L(\boldsymbol{x}, \boldsymbol{v})}{\partial \boldsymbol{v}} = \frac{m\boldsymbol{v}}{\sqrt{1 - \frac{v^2}{c^2}}}. \tag{1.6}$$

Then the relativistic free particle Hamiltonian $H \equiv H(\boldsymbol{x}, \boldsymbol{p})$ is

$$H = c\sqrt{m^2c^2 + \boldsymbol{p}^2}. \tag{1.7}$$

The Hamiltonian for a particle in the presence of external fields that are determined by a scalar potential $\varphi(\boldsymbol{x})$ and a vector potential $\boldsymbol{A}(\boldsymbol{x})$ is acquired from Eq. (1.7) by using the minimal coupling substitution,[1] hence

$$H = c\sqrt{m^2c^2 + \boldsymbol{\pi}^2} + q\varphi(\boldsymbol{x}), \tag{1.8}$$

where

$$\boldsymbol{\pi} = \boldsymbol{p} - q\boldsymbol{A}(\boldsymbol{x}) \tag{1.9}$$

is the canonical momentum, and q is the particle's charge.

1.1.2 Quantization

Presence of the square root in the relativistic Hamiltonian in Eq. (1.8) makes construction of a relativistic quantum theory far from straightforward. Dirac sought an equation that is linear in space and time, and proposed a strategy based on the assumption, that the expression under the

[1] Alternatively, we could introduce the generalized potential energy into the relativistic Lagrangian in Eq. (1.5) to obtain the Lagrangian of a relativistic charged particle in the presence of external fields:

$$L(\boldsymbol{x}, \boldsymbol{v}) = -mc^2\sqrt{1 - \frac{v^2}{c^2}} - q\varphi(\boldsymbol{x}) + q\dot{\boldsymbol{x}} \cdot \boldsymbol{A}(\boldsymbol{x}).$$

This Lagrangian would directly yield the Hamiltonian in Eq. (1.8), justifying the use of the minimal coupling substitution.

square root can be written as a perfect square[4]

$$m^2c^2 + \boldsymbol{\pi}^2 = (\boldsymbol{\alpha} \cdot \boldsymbol{\pi} + \beta mc)^2 \tag{1.10}$$

for some unknown parameters $\boldsymbol{\alpha}$ and β. In order for the assumption in Eq. (1.10) to be valid, the parameters $\boldsymbol{\alpha}$ and β must satisfy the following relations:

$$\beta^2 = 1, \tag{1.11a}$$
$$\alpha_i\beta + \beta\alpha_i = 0, \tag{1.11b}$$
$$\alpha_i\alpha_j + \alpha_j\alpha_i = 2\delta_{ij}, \tag{1.11c}$$

for $i = 1, 2, 3$, where δ_{ij} is the Kronecker delta. Clearly, these equations imply that $\boldsymbol{\alpha}$ and β must anticommute, and thus they cannot belong to a commutative algebra, such as algebras of real or complex numbers. Within matrix algebra, Eqs. (1.11) can be satisfied by the 4×4 matrices

$$\boldsymbol{\alpha} = \begin{pmatrix} \mathbf{0}_2 & \boldsymbol{\sigma} \\ \boldsymbol{\sigma} & \mathbf{0}_2 \end{pmatrix}, \qquad \beta = \begin{pmatrix} \mathbb{I}_2 & 0_2 \\ 0_2 & -\mathbb{I}_2 \end{pmatrix}, \tag{1.12}$$

where $\boldsymbol{\sigma}$ is the vector of the Pauli matrices, 0_2 is the 2×2 zero matrix, and $\mathbb{I}_2$ is the 2×2 unit matrix. From the multiplication rule of the Pauli matrices, it follows that

$$\alpha_i\alpha_j = \delta_{ij}\mathbb{I}_4 + i\varepsilon_{ijk}\Sigma_k, \tag{1.13}$$

where ε_{ijk} is the Levi-Civita symbol, $\boldsymbol{\Sigma} \equiv \mathbb{I}_2 \otimes \boldsymbol{\sigma}$ is the 4-component spin operator, $\otimes$ denotes the tensor product of matrices, and i is the complex unit.

In principle, to satisfy the perfect square in Eq. (1.10), it is sufficient that $\alpha_i\alpha_j = \delta_{ij}$, because it gives $(\boldsymbol{\alpha} \cdot \boldsymbol{\pi})^2 = \boldsymbol{\pi}^2$. However, the correct quantum-mechanical interaction of the magnetic field with the electron spin represented by the Pauli matrices $\boldsymbol{\sigma}$ is only obtained when the full expression in Eq. (1.13) is used:

$$(\boldsymbol{\alpha} \cdot \boldsymbol{\pi})^2 = \boldsymbol{\pi}^2 - q\boldsymbol{\Sigma} \cdot \boldsymbol{B}, \tag{1.14}$$

where $\boldsymbol{B} = \boldsymbol{\nabla} \times \boldsymbol{A}$ is the magnetic field.

1.1.3 Time-dependent Dirac equation

Let us insert Eq. (1.10) into the Hamiltonian in Eq. (1.8), and quantize the position and the momentum according to the correspondence principle. Let $V(\boldsymbol{r}) \equiv q\varphi(\boldsymbol{r})$ denote the scalar potential (in energy units). Furthermore, let us substitute $m = 1$ and $q = -1$ for the electron rest mass and charge in atomic units, respectively. Then the time-dependent Dirac equation is

$$i\frac{\partial\psi}{\partial t} = h_{\mathrm{D}}\psi, \tag{1.15}$$

where

$$\boxed{h_{\mathrm{D}} = c\boldsymbol{\alpha}\cdot\boldsymbol{\pi} + \beta c^2 + V(\boldsymbol{r})} \tag{1.16}$$

is the one-electron Dirac Hamiltonian,

$$\boldsymbol{\pi} = -i\boldsymbol{\nabla} + \boldsymbol{A}(\boldsymbol{r}) \tag{1.17}$$

is the electron's canonical momentum operator,[2] and

$$\psi \equiv \psi(\boldsymbol{r}, t) = \begin{pmatrix}\psi^L(\boldsymbol{r}, t)\\ \psi^S(\boldsymbol{r}, t)\end{pmatrix} \tag{1.18}$$

is the 4-component wave function of the electron; ψ^L and ψ^S being the large (L) and small (S) spinor components of the wave function, respectively. Contrary to the Schrödinger equation, the one-electron Dirac equation remains invariant under a Lorentz transformation, and thus constitutes a relativistic extension of the nonrelativistic quantum mechanics. In the relativistic quantum chemistry schemes that employ 4-component Dirac-type equations, and 4-component wave functions and operators, are referred to as *4-component* (4c) methods. The methods that approximate the Dirac equation by eliminating the small-component wave function, establishing 2-component wave functions are described as *2-component* (2c). Nonrelativistic methods based on the Schrödinger equation are called *1-component* (1c) methods.

The Dirac equation can be used to express the electron density and current density using 4c wave functions. Multiplying Eq. (1.15) from the left with Hermitian conjugate of the wave function $\psi^\dagger$ gives

$$i\psi^\dagger\frac{\partial\psi}{\partial t} = \psi^\dagger\left(c\boldsymbol{\alpha}\cdot(-i\boldsymbol{\nabla} + \boldsymbol{A}(\boldsymbol{r})) + \beta c^2 + V(\boldsymbol{r})\right)\psi.$$

[2] The version of $\boldsymbol{\pi}$ that is used here is different than in Eq. (1.9), I assume it should be clear from the context, which $\boldsymbol{\pi}$ is used.

Adding this equation to its Hermitian conjugate we obtain the continuity equation

$$\frac{\partial \rho}{\partial t} + \boldsymbol{\nabla} \cdot \boldsymbol{j} = 0, \tag{1.19}$$

where we defined the *electron probability density* ρ and the *probability current density* $\boldsymbol{j}$ as

$$\rho(\boldsymbol{r}, t) \equiv \psi^\dagger(\boldsymbol{r}, t)\psi(\boldsymbol{r}, t), \tag{1.20}$$

$$\boldsymbol{j}(\boldsymbol{r}, t) \equiv \psi^\dagger(\boldsymbol{r}, t)c\boldsymbol{\alpha}\psi(\boldsymbol{r}, t). \tag{1.21}$$

Note that the relativistic 4c expression for the current density is formally simpler than its nonrelativistic counterpart (omitting the arguments $(\boldsymbol{r}, t)$)

$$\boldsymbol{j}_{\text{n.r.}} = \frac{1}{2i}\Big(\psi^*(\boldsymbol{\nabla}\psi) - \psi(\boldsymbol{\nabla}\psi^*)\Big) \tag{1.22}$$

for a 1c wave function ψ, where the star $(^*)$ indicates complex conjugation.

1.1.4 Time-independent Dirac equation

In analogy with the nonrelativistic case, the time-independent Dirac equation takes the form of

$$h_{\text{D}}\psi_n = \varepsilon_n \psi_n, \tag{1.23}$$

where $\psi_n \equiv \psi_n(\boldsymbol{x})$ are the stationary states and ε_n are their energies. Since the Dirac Hamiltonian is not bounded from below, solutions of Eq. (1.23) constitute two sets, separated by an energy gap[3] $\Delta \approx 2c^2$. The sets are referred to as the *positive-energy* and the *negative-energy* states. To obtain energies of the electronic states that are directly comparable with the nonrelativistic energies, it is a common practice to shift the energy scale of the Dirac Hamiltonian by c^2. Then the Dirac Hamiltonian becomes

$$\boxed{h_{\text{D}} = \begin{pmatrix} V(\boldsymbol{r}) & c\boldsymbol{\sigma}\cdot\boldsymbol{\pi} \\ c\boldsymbol{\sigma}\cdot\boldsymbol{\pi} & V(\boldsymbol{r}) - 2c^2 \end{pmatrix}}. \tag{1.24}$$

Such a shift only changes the global phase of the wave function, and hence has no physical meaning.

[3] This gap *exactly* equals $2c^2$ in the absence of external potentials V and $\boldsymbol{A}$. Inclusion of the Coulomb potential from the nucleus in the Dirac equation gives rise to bound states with energies located inside the gap, but close to its upper (and lower) boundary. As a consequence, the gap is slightly shrunk.

1.2 Restricted kinetic balance

In order to solve Eq. (1.23) for given potentials V and $\boldsymbol{A}$, eigenfunctions ψ_n must be represented in an approximate manner. One such common representation is an expansion in a given fixed basis composed of some known functions $\chi_\mu(\boldsymbol{r})$. Such an expansion is exact in principle, but in computer implementations the expansion must be truncated, giving rise to numerical errors. In the context of relativistic methods, the 4c Dirac Hamiltonian in Eq. (1.24) couples the large and small component of the wave functions. Early finite basis calculations using the Dirac Hamiltonian were hindered by convergence problems,[40,41] because the basis did not respect this coupling.[42,43] The coupling condition can be seen by writing Eq. (1.23) as

$$V(\boldsymbol{r})\psi^L + c\boldsymbol{\sigma}\cdot\boldsymbol{p}\psi^S = \varepsilon\psi^L, \tag{1.25a}$$

$$c\boldsymbol{\sigma}\cdot\boldsymbol{p}\psi^L + \left(V(\boldsymbol{r}) - 2c^2\right)\psi^S = \varepsilon\psi^S, \tag{1.25b}$$

where we omitted the vector potential for clarity, and dropped the index n. We can express the small component ψ^S from the second equation as

$$c\psi^S = \frac{1}{2}\frac{\boldsymbol{\sigma}\cdot\boldsymbol{p}}{\frac{\varepsilon - V(\boldsymbol{r})}{2c^2} + 1}\psi^L \sim \frac{1}{2}\boldsymbol{\sigma}\cdot\boldsymbol{p}\psi^L \quad (\text{as } c\to\infty). \tag{1.26}$$

If we insert this expression in the limit of $c\to\infty$ to Eq. (1.25a), we immediately recover the nonrelativistic Schrödinger equation. However, this is only true for a complete (infinitely large) basis. To obtain a correct nonrelativistic limit of the kinetic energy operator in an incomplete basis, Stanton and Havriliak suggested to employ the condition in Eq. (1.26) at the basis level[35]. This means that the small-component basis functions χ^S_μ are generated from the large-component basis functions χ^L_μ as

$$\boxed{\chi^S_\mu(\boldsymbol{r}) = \frac{1}{2c}\boldsymbol{\sigma}\cdot\boldsymbol{p}\chi^L_\mu(\boldsymbol{r})}. \tag{1.27}$$

The condition in Eq. (1.27) is referred to as *restricted kinetic balance* (RKB), and was later generalized to incorporate a nonzero vector potential $\boldsymbol{A}$ in the study of magnetic properties.[44]

1.3 Modified Dirac equation

From now on we shall assume that $\boldsymbol{A} = \boldsymbol{0}$, omitting the vector potential from the following discussions. A 4c wave function $\psi(\boldsymbol{r})$ is expanded using 4c basis functions $\chi_\mu(\boldsymbol{r})$ as

$$\psi(\boldsymbol{r}) = \chi_\mu(\boldsymbol{r})c^\mu, \tag{1.28}$$

where

$$\chi_\mu(\boldsymbol{r}) = \begin{pmatrix} \chi_\mu^L(\boldsymbol{r}) & 0_2 \\ 0_2 & \chi_\mu^S(\boldsymbol{r}) \end{pmatrix} \tag{1.29}$$

is a 4×4 matrix of basis functions, and $c^\mu \equiv (c_L^\mu, c_S^\mu)^T$ is a 4c vector of expansion coefficients. Letting $g_\mu(\boldsymbol{r})$ denote scalar basis functions, we construct χ_μ^L and χ_μ^S to satisfy the RKB condition in Eq. (1.27), hence

$$\chi_\mu^L(\boldsymbol{r}) = \mathbb{I}_2 \otimes g_\mu(\boldsymbol{r}), \tag{1.30a}$$

$$\chi_\mu^S(\boldsymbol{r}) = \frac{1}{2c}\boldsymbol{\sigma} \cdot \boldsymbol{p} g_\mu(\boldsymbol{r}). \tag{1.30b}$$

If we insert the expansion in Eq. (1.28) into the time-independent Dirac Eq. (1.23), apply $\chi_{\mu'}^\dagger(\boldsymbol{r})$ from the left, and integrate over the spacial coordinates $\boldsymbol{r}$, then we obtain the matrix form of the Dirac equation

$$\boxed{\begin{pmatrix} \mathcal{V}^{LL} & \mathcal{T} \\ \mathcal{T} & \frac{1}{4c^2}\mathcal{V}^{SS} - \mathcal{T} \end{pmatrix} \begin{pmatrix} c_L \\ c_S \end{pmatrix} = \varepsilon \begin{pmatrix} \mathcal{S} & 0_2 \\ 0_2 & \frac{1}{2c^2}\mathcal{T} \end{pmatrix} \begin{pmatrix} c_L \\ c_S \end{pmatrix}}, \tag{1.31}$$

where

$$\mathcal{S}_{\mu\mu'} = \mathbb{I}_2 \otimes \int g_\mu^*(\boldsymbol{r}) g_{\mu'}(\boldsymbol{r}) d^3\boldsymbol{r}, \tag{1.32a}$$

$$\mathcal{T}_{\mu\mu'} = \mathbb{I}_2 \otimes \int g_\mu^*(\boldsymbol{r}) \frac{p^2}{2} g_{\mu'}(\boldsymbol{r}) d^3\boldsymbol{r}, \tag{1.32b}$$

$$\mathcal{V}_{\mu\mu'}^{LL} = \mathbb{I}_2 \otimes \int g_\mu^*(\boldsymbol{r}) V(\boldsymbol{r}) g_{\mu'}(\boldsymbol{r}) d^3\boldsymbol{r}, \tag{1.32c}$$

$$\mathcal{V}_{\mu\mu'}^{SS} = \int g_\mu^*(\boldsymbol{r}) (\boldsymbol{\sigma} \cdot \boldsymbol{p}) V(\boldsymbol{r}) (\boldsymbol{\sigma} \cdot \boldsymbol{p}) g_{\mu'}(\boldsymbol{r}) d^3\boldsymbol{r}, \tag{1.32d}$$

Matrix Eq. (1.31) is referred to as the *modified Dirac equation*.[45] Since the speed of light only appears in the denominator, the nonrelativistic limit can simply be obtained by putting $c \to \infty$, which gives $c_L = c_S$ and, subsequently, the Schrödinger equation.

One of the advantages of Eq. (1.31) is that we can isolate the scalar-relativistic spin-free contributions from the terms that couple various spin components. The only non-scalar terms arise from the small-component potential $\mathcal{V}^{SS}_{\mu\mu'}$ defined in Eq. (1.32d). Applying the multiplication rule of the Pauli matrices on the operator $(\boldsymbol{\sigma}\cdot\boldsymbol{p})V(\boldsymbol{r})(\boldsymbol{\sigma}\cdot\boldsymbol{p})$ yields

$$(\boldsymbol{\sigma}\cdot\boldsymbol{p})V(\boldsymbol{\sigma}\cdot\boldsymbol{p}) = \boldsymbol{p}V\cdot\boldsymbol{p} + (\boldsymbol{p}V\times\boldsymbol{p})\cdot i\boldsymbol{\sigma}. \tag{1.33}$$

From this equation we can see, that only the second term is non-diagonal in the spin space. This term is responsible for the spin–orbit coupling (SOC), and neglecting it results in the scalar relativistic form of the Dirac equation.[46] Note, that because of the SOC term, the Dirac Hamiltonian does not commute with the total spin operator[4] $\boldsymbol{s} \equiv \mathrm{diag}(\boldsymbol{\sigma}/2, \boldsymbol{\sigma}/2)$.

1.4 Time reversal symmetry

The concept of time reversal (TR) symmetry plays a central role in the works included in this thesis [**Paper I**–**V**]. Therefore, here I provide a short summary of the main definitions and results that are then build on in our articles.

Let $\mathcal{K}$ denote the 4c one-electron TR operator. $\mathcal{K}$ is required to change the sign of the momentum operator, but leave the position operator unchanged, hence

$$\mathcal{K}\boldsymbol{r}\mathcal{K}^\dagger = \boldsymbol{r}, \qquad \mathcal{K}\boldsymbol{p}\mathcal{K}^\dagger = -\boldsymbol{p}. \tag{1.34}$$

Consequently, the angular momentum operator $\boldsymbol{l} \equiv \boldsymbol{r}\times\boldsymbol{p}$ and the 4c spin operator $\boldsymbol{s} \equiv \boldsymbol{\Sigma}/2$ transform as

$$\mathcal{K}\boldsymbol{l}\mathcal{K}^\dagger = -\boldsymbol{l}, \qquad \mathcal{K}\boldsymbol{s}\mathcal{K}^\dagger = -\boldsymbol{s}. \tag{1.35}$$

It follows for the $\boldsymbol{\alpha}$ and β matrices that

$$\mathcal{K}\boldsymbol{\alpha}\mathcal{K}^\dagger = -\boldsymbol{\alpha}, \qquad \mathcal{K}\beta\mathcal{K}^\dagger = \beta. \tag{1.36}$$

Demanding that $\mathcal{K}$ is a linear operator leads to a contradiction of Eqs. (1.34) with the canonical commutation relation $[x_i, p_j] = i\delta_{ij}$. The problem is re-

[4] This definition of the spin operator trivially extends the standard 2c definition $\boldsymbol{\sigma}/2$.

solved by defining $\mathcal{K}$ as an *antilinear*, and *antiunitary* operator.[5] An explicit form of $\mathcal{K}$ that satisfies the desired properties can be written as[37,47,48]

$$\mathcal{K} = -i \begin{pmatrix} \sigma_y & 0_2 \\ 0_2 & \sigma_y \end{pmatrix} \mathcal{K}_0, \tag{1.37}$$

where $\mathcal{K}_0$ denotes the complex conjugation operator. It follows from this definition that

$$\mathcal{K}^\dagger = -\mathcal{K}, \tag{1.38a}$$
$$\mathcal{K}^\dagger \mathcal{K} = \mathbb{I}_4. \tag{1.38b}$$

The conditions in Eqs. (1.34) and (1.36) imply ($[\cdot,\cdot]$ denotes the commutator.)

$$[\mathcal{K}, h_\mathrm{D}] = 0 \tag{1.39}$$

for the Dirac Hamiltonian h_D in absence of magnetic fields ($\boldsymbol{A} = \boldsymbol{0}$). Applying $\mathcal{K}$ to the time-dependent Dirac Eq. (1.15) from the left, and using Eq. (1.39), we prove the following theorem:

Theorem 1. *Let $\psi(\boldsymbol{r},t) \equiv \psi$ be a solution to the time-dependent Dirac equation $i\frac{\partial\psi}{\partial t} = h_D\psi$, where $h_D = c\boldsymbol{\alpha}\cdot\boldsymbol{p} + \beta c^2 + V(\boldsymbol{r})$. Then $\bar{\psi}(\boldsymbol{r},t) \equiv \mathcal{K}\psi(\boldsymbol{r},-t)$ is a solution of the same equation.*

Similarly, letting $\mathcal{K}$ act on the time-independent Dirac Eq. (1.23), we can prove:

Theorem 2 (Kramers)**.** *Let $\psi(\boldsymbol{r}) \equiv \psi$ be a solution to the time-independent Dirac equation $h_D\psi = \varepsilon\psi$, where $h_D = c\boldsymbol{\alpha}\cdot\boldsymbol{p} + \beta c^2 + V(\boldsymbol{r})$. Then $\bar{\psi}(\boldsymbol{r}) \equiv \mathcal{K}\psi(\boldsymbol{r})$ is a solution with the same energy ε. In addition, ψ and $\bar{\psi}$ are orthogonal,* i.e. $\langle\bar{\psi}|\psi\rangle = 0$.

[5] An operator K is called *antilinear* iff

$$K(af + bg) = a^* Kf + b^* Kg$$

for arbitrary complex numbers $a, b \in \mathbb{C}$ and functions (vectors) f, g. In addition, iff $K^\dagger K = \mathbb{I}$, then K is called antiunitary. Compared to linear operators, Hermitian conjugation of an antilinear operator is defined with an extra complex conjugation, hence

$$(f, Kg) = (K^\dagger f, g)^*,$$

where $(\cdot,\cdot)$ denotes an inner product.

Proof. The first part follows from Eq. (1.39). To prove the orthogonality, consider:

$$-\langle \mathcal{K}\psi|\psi\rangle = \langle \mathcal{K}\psi|\mathcal{K}^2\psi\rangle = \langle \mathcal{K}^\dagger\mathcal{K}\psi|\mathcal{K}\psi\rangle^* = \langle\psi|\mathcal{K}\psi\rangle^* = \langle \mathcal{K}\psi|\psi\rangle\,.$$

□

According to Theorem 2, eigenstates of the one-electron Dirac Hamiltonian are doubly degenerate.[6] Therefore, we can compose a symmetry-adapted basis consisting of pairs $\{|p\rangle\,, |\bar{p}\rangle\}$, where $|\bar{p}\rangle \equiv \mathcal{K}\,|p\rangle$. Such pairs of two time-reversal related states are called *Kramers partners*. An operator A is called TR-symmetric iff it commutes with $\mathcal{K}$, *i.e.*

$$[A, \mathcal{K}] = 0. \tag{1.40}$$

TR-symmetric operators acquire a special structure when expressed in the basis of Kramers pairs.[47–51] This can be seen by evaluating elements of a TR-symmetric operator A. Let $a \equiv \langle p|A|p\rangle$ and $b \equiv \langle p|A|\bar{p}\rangle$ denote 2 distinct elements of A. It follows for the 2 remaining elements, that

$$\langle \bar{p}|A|p\rangle = \langle \mathcal{K}p|A|p\rangle = \langle p|\mathcal{K}^\dagger A|p\rangle^* = -\langle p|\mathcal{K}A|p\rangle^* = -\langle p|A\mathcal{K}|p\rangle^* = -b^*$$

and

$$\langle \bar{p}|A|\bar{p}\rangle = \langle p|\mathcal{K}^\dagger A\mathcal{K}|p\rangle^* = \langle p|A\mathcal{K}^\dagger\mathcal{K}|p\rangle^* = \langle p|A|p\rangle^* = a^*.$$

Therefore, the operator A can be written as

$$\boxed{A = \begin{bmatrix} a & b \\ -b^* & a^* \end{bmatrix}}. \tag{1.41}$$

A matrix that has the TR-symmetric structure of Eq. (1.41) can compactly be decomposed using a matrix basis consisting of the Pauli matrices times the imaginary unit i and the identity matrix. Hence

$$A = \sum_{q=0}^{3} A^q e_q \equiv A^q e_q, \tag{1.42}$$

[6] In fact, this is true for any system with half-integer total spin described by a TR-symmetric Hamiltonian.

where

$$A^0 = \mathrm{Re}\, a, \qquad e_0 = \mathbb{I}_2, \tag{1.43a}$$
$$A^1 = \mathrm{Im}\, a, \qquad e_1 = i\sigma_z, \tag{1.43b}$$
$$A^2 = \mathrm{Re}\, b, \qquad e_2 = i\sigma_y, \tag{1.43c}$$
$$A^3 = \mathrm{Im}\, b, \qquad e_3 = i\sigma_x. \tag{1.43d}$$

Such a decomposition enables encoding of 4 complex-matrix elements of TR-symmetric operators using 4 real-valued elements A^q. The decomposition in Eq. (1.42) provides a non-redundant framework for 2c and 4c operators, and can be exploited to greatly reduce computational effort when constructing these operators. For more complicated operators[7] the computational savings can exceed the obvious factor of 2. Adaptations of this scheme in a more general context of complex A^q are shown and discussed in **Paper IV** and **V**.

1.5 Two-component Hamiltonians

The study of molecules and solids within the framework of self-consistent field (SCF) theory poses a twofold computational challenge: Construction of an effective one-electron Hamiltonian and its subsequent diagonalization. Inclusion of relativistic effects at the 4c level of theory increases computational complexity for both these SCF steps. For this reason, approximations that circumvent the need to compose the full 4c Dirac Hmailtonian are sought.

Perhaps the most obvious way to eliminate the small component wave function ψ^S is to insert the exact expression for ψ^S in Eq. (1.26) to Eq. (1.25a):

$$V(\boldsymbol{r})\psi^L + \frac{1}{2}\boldsymbol{\sigma}\cdot\boldsymbol{p}R(\varepsilon)\boldsymbol{\sigma}\cdot\boldsymbol{p}\psi^L = \varepsilon\psi^L, \tag{1.44}$$

where

$$R(\varepsilon) = \left(1 + \frac{\varepsilon - V(\boldsymbol{r})}{2c^2}\right)^{-1}. \tag{1.45}$$

Expanding $R(\varepsilon) \approx 1 - \frac{\varepsilon - V(\boldsymbol{r})}{2c^2}$ and correcting the norm of the large compo-

[7] Such as the Coulomb mean-field or exchange–correlation contributions to the potential, see Chapter 2.

nent ψ^L yields an approximate 2c Pauli Hamiltonian

$$h_{\mathrm{P}} = \frac{p^2}{2} + V - \frac{p^4}{8c^2} + \frac{1}{8c^2}(\nabla^2 V) + \frac{1}{4c^2}\left[(\boldsymbol{\nabla} V) \times \boldsymbol{p}\right] \cdot \boldsymbol{\sigma} \tag{1.46}$$

used when it is sufficient to treat the relativistic effects perturbationally.[8] Shortcomings of the Pauli Hamiltonians can be circumvented by developing the zeroth-order regular approximation (ZORA) to the coupling.[52–54] This approximation leads to a variationally stable ZORA Hamiltonian

$$h_{\mathrm{ZORA}} = V + \frac{1}{2}(\boldsymbol{\sigma} \cdot \boldsymbol{p})\frac{2c^2}{2c^2 - V}(\boldsymbol{\sigma} \cdot \boldsymbol{p}). \tag{1.47}$$

However, the appearance of the potential V in the denominator hinders analytical evaluation of the Hamiltonian in a finite basis, and numerical integration schemes are preferred.

Alternatively, a unitary Foldy–Wouthuysen-type transformation[55] that block-diagonalizes the Dirac Hamiltonian can be composed. The matrix formulation of such a transformation leads to the *exact 2-component* (X2C) Hamiltonian.[56–58] An application of the X2C procedure to many-electron problems involves in its simplest form the one-electron Dirac Hamiltonian. Its eigenvectors are then used to find an explicit form of the decoupling matrix U. The matrix U is parameterized as

$$U = \begin{pmatrix} (1 + R^\dagger R)^{-1/2} & 0 \\ 0 & (1 + RR^\dagger)^{-1/2} \end{pmatrix} \begin{pmatrix} 1 & -R^\dagger \\ R & 1 \end{pmatrix}, \tag{1.48}$$

where R is a 2×2 matrix determined by requiring that[58]

$$U \begin{pmatrix} c_+^L & c_-^L \\ c_+^S & c_-^S \end{pmatrix} = \begin{pmatrix} \tilde{c}_+ & 0 \\ 0 & \tilde{c}_- \end{pmatrix}, \tag{1.49}$$

which is equivalent to requiring that U block-diagonalizes the one-electron Dirac Hamiltonian h_{D}. Here we denoted the positive-energy and negative-energy matrix blocks with $+$ and $-$, respectively. This leads to the linear matrix equations

$$c_-^L - R^\dagger c_-^S = 0, \tag{1.50a}$$

$$R c_+^L + c_+^S = 0, \tag{1.50b}$$

[8] The variational approach is hindered by the presence of the $-p^4$ operator which makes the Pauli Hamiltonian unbounded from below.

that are solved to find R. Computational savings are obtained by removing the negative-energy blocks from the subsequent SCF procedure, giving rise to an *approximate* 2c method. In addition to reducing the number of the wave function components to 2, such a scheme avoids evaluation of expensive two-electron terms in the 4c basis. In **Paper III** and **IV** we extend this X2C approach to the time-dependent SCF in the study of relativistic effects on time-dependent response properties.

1.6 Interacting electrons

So far our discussion only involved the one-electron Dirac Hamiltonain. However, in molecular and condensed-matter systems, electron–electron interactions cannot be neglected. We could now shift our focus to QED, which is the Lorentz invariant quantum theory of electrons, positrons and photons. Such an approach would require introducing concepts of quantum field theory, and would result in equations that are immensely complicated to solve for polyatomic systems. The difficulties can vastly be mitigated by realizing that some QED processes, such as the electron–positron pair creation, are not relevant for the low-energy range that is of interest in molecular and condensed-matter sciences.[38]

The electromagnetic (photon) field can be split into an *external* field and an *internal* field. The external field contains the interaction of electrons with nuclei as well as various electric and magnetic fields that are introduced when studying response properties. The internal electromagnetic field describes electron–electron interactions, and is approximated by the nonrelativistic instantaneous Coulomb interaction. The described process yields the many-electron Hamiltonian known as the Dirac–Coulomb Hamiltonian that takes the following form:

$$H = \sum_{i=1}^{N_\mathrm{e}} h_\mathrm{D}(i) + \frac{1}{2} \sum_{i,j\neq i}^{N_\mathrm{e}} g(i,j), \tag{1.51}$$

where

$$h_{\mathrm{D}}(i) = \begin{pmatrix} V(\boldsymbol{r}_i) & c\boldsymbol{\sigma}_i \cdot \boldsymbol{\pi}_i \\ c\boldsymbol{\sigma}_i \cdot \boldsymbol{\pi}_i & V(\boldsymbol{r}_i) - 2c^2 \end{pmatrix}, \tag{1.52}$$

$$g(i,j) = \frac{\mathbb{I}_4 \otimes \mathbb{I}_4}{|\boldsymbol{r}_i - \boldsymbol{r}_j|}, \tag{1.53}$$

$$\boldsymbol{\pi}_i = \boldsymbol{p}_i + \boldsymbol{A}(\boldsymbol{r}_i), \tag{1.54}$$

$\boldsymbol{r}_i$ and $\boldsymbol{p}_i$ are the position and momentum operators of the i-th electron, respectively, $\boldsymbol{\sigma}_i$ are Pauli matrices for the i-th electron, and N_{e} denotes the total number of electrons. Note, that the Dirac–Coulomb Hamiltonian is not Lorentz invariant.

In this entire work we use the Dirac–Coulomb Hamiltonain in the context of Hartree–Fock (HF) theory and density functional theory (DFT). An additional relativistic two-electron term – the Breit operator[59,60] – can be introduced to the two-electron Hamiltonian in Eq. (1.53). However, such an approach would require an extension of conventional density functionals to incorporate dependence on the current density,[61] and is usually not necessary when studying molecular systems and solids.

Chapter 2

Self-consistent field theory

> If you are receptive and humble, mathematics will lead you by the hand.
>
> *Paul Dirac*

Practical calculations of electronic structure and response properties of molecules and solids must always involve a set of sophisticated approximations. In principle, one should solve the Schrödinger (or Dirac–Coulomb) equation with the many-body Hamiltonian acting on the many-body wave function. Such a wave function depends on coordinates (and spin) of *all* electrons and nuclei, and the associated equation is immensely complicated to solve. The problem is significantly simplified by assuming the Born–Oppenheimer approximation, which enables decoupling of the electronic and nuclear degrees of freedom.[62] This common approximation stems from the fact that nuclei are much heavier than electrons, and is employed here as well as the included works [**Paper I**–**V**]. As a consequence, it is sufficient to limit our discussion to the *electronic* Hamiltonian, that depends *parametrically* on the nuclear coordinates.[1] The many-electron Hamiltonian adopted in this work takes the form of the Dirac–Coulomb Hamiltonian in Eq. (1.51), and acts on the many-electron multi-component wave function.

The many-electron Schrödinger equation is still far too complicated to solve for realistic systems, and electronic structure theory provides a

[1] The Born–Oppenheimer approximation justifies our restriction to the electronic Hamiltonian when discussing the relativistic theory in Chapter 1.

plethora of approximate methods to obtain the ground state wave function and energy. I refer the interested reader to the book of Helgaker, Jørgensen and Olsen,[63] and the book of Piela[64] for more information about these methods. In this work we restrict ourselves to the methods based on self-consistent field (SCF) theory, where the many-electron problem is replaced by a set of *effective* one-electron problems.

The rest of this chapter contains an overview of key principles that are required to formulate relativistic SCF methods. These principles are expanded to the time domain in a study of real-time electron dynamics in **Paper I**–**IV**, and applied to band-structure calculations of materials in the solid state in **Paper V**. These topics will be introduced in Chapters 3 and 4.

2.1 Hartree–Fock and Kohn–Sham

Effective one-electron equations can be constructed by approximating the many-electron wave function with a single Slater determinant consisting of several one-electron wave functions, called *spinorbitals*. These spinorbitals are determined variationally to minimize the total energy of the system. The variational principle together with the single-determinant ansatz for the wave function yield a set of nonlinear equations for the unknown spinorbitals, known as the Hartree–Fock (HF) equations. If no assumption is made for the spin components of the spinorbitals, the HF method is then called the *general* HF (GHF) method, in which the spinorbitals are complex functions with mixed spin components.[2] The major downside of the HF method is that it does not account for electron correlation, *i.e.* that the true many-electron wave function should be represented as a linear combination of Slater determinants. Post-HF methods mitigate the lack of electron correlation in the HF method at the expense of great computational effort.

A conceptually very different approach is based on Kohn–Sham (KS) density functional theory (DFT),[65,66] and its relativistic extension.[67] DFT

[2]Compared to the *unrestricted* HF (UHF), where we assume that the individual components of the spinorbitals are real functions, and that there is no mixing of the spin components, *i.e.* all spinorbitals contain exactly *one* nonzero spin component. Within the UHF method, there are two sets of spatial functions (*orbitals*), one for each spin component. *Restricted* HF (RHF) additionally assumes, that the orbitals for both spin components are identical. See Piela,[64] for example.

provides a principally exact mapping between the many-electron wave function and a much simpler object: the electron (probability) density ρ. The total energy E is then written as a functional of the electron density

$$E[\rho] = \int \rho(\boldsymbol{r}) v(\boldsymbol{r}) d^3\boldsymbol{r} + F[\rho], \tag{2.1}$$

$$F[\rho] = T[\rho] + U[\rho], \tag{2.2}$$

where $T[\rho]$ is the kinetic energy functional, $U[\rho]$ is the electron–electron interaction energy functional, and v is the external potential, containing electron–nuclear attraction. Unfortunately, the exact expression for the $F[\rho]$ functional (called the universal functional) in Eq. (2.2) is not known, and hence must be modeled. Kohn and Sham introduced a fictitious system of non-interacting electrons moving in an effective external potential, constructed so that the fictitious system has the same electron density as the real interacting system.[66] The system is described by a set of effective one-electron equations (the KS equations) that are formally similar to the HF equations. The problem of the unknown kinetic energy functional $T[\rho]$ is partially alleviated, because expressing the kinetic energy of the non-interacting system KS T_0 is straightforward, leaving only the difference $T - T_0$ undetermined. The terms in the energy functional are rearranged as

$$E[\rho] = T_0[\rho] + \int \rho(\boldsymbol{r}) v(\boldsymbol{r}) d^3\boldsymbol{r} + E_{\mathrm{H}}[\rho] + E_{\mathrm{xc}}[\rho], \tag{2.3}$$

$$E_{\mathrm{xc}}[\rho] = T[\rho] - T_0[\rho] + U[\rho] - E_{\mathrm{H}}[\rho], \tag{2.4}$$

where

$$E_{\mathrm{H}}[\rho] = \frac{1}{2} \iint \frac{\rho(\boldsymbol{r}_1)\rho(\boldsymbol{r}_2)}{|\boldsymbol{r}_1 - \boldsymbol{r}_2|} d^3\boldsymbol{r}_1 d^3\boldsymbol{r}_2 \tag{2.5}$$

is the Hartree (or Coulomb) energy functional, and $E_{\mathrm{xc}}[\rho]$ is the exchange–correlation (XC) energy. $T_0[\rho]$ is understood as an *implicit* functional of the density, obtained from the solutions of the KS equations. The main advantage of the KS approach is that the first four terms in Eq. (2.3) are known explicitly, and are inexpensive to calculate, while only the XC energy remains to be determined. E_{xc} is typically much smaller than the three other terms, and is modeled using local density approximation[68,69] (LDA), generalized gradient approximation[70] (GGA), or hybrid functionals[71] that contain the HF exact exchange admixture. There are more cases of the density functionals; the hierarchy of various approximations for the functional ("Jacob's ladder") can be found in the work of Perdew and Schmidt.[72]

Despite having very different origins, the resulting HF and KS equations are similar at a practical level, and we refer to them commonly as the SCF equations. 4c variants of the HF and KS equations are called the Dirac–Hartree–Fock (DHF) and Dirac–Kohn–Sham (DKS) equations to explicitly highlight that the nonrelativistic one-electron Hamiltonian is replaced by the 4c Dirac Hamiltonian in Eq. (1.24). Owing to the one-electron nature of the KS equations, KS DFT facilitates incorporation of electron correlation effects roughly at the cost of the HF method, which is in contrast to post-HF methods.

2.2 Density matrices

There are multiple ways of encoding information about a state of a system in quantum mechanics. Representing the state with the many-electron wave function can be somewhat cumbersome, and as we will see here, expectation values of many operators only require knowledge of simpler, quantities called *reduced density matrices*. The excellent book of McWeeny[36] covers the broad topic of the density matrices and their applications in various subfields of molecular quantum mechanics. The reduced density matrices can be defined either as integrals of the many-electron wave function, or using the occupation number representation (also known as "second quantization"). Here we employ the second-quantized formulation,[36,63] which allows us to obtain expressions directly in a discrete basis (such as atomic orbitals).

Let H denote a many-electron Hamiltonian [for instance the Dirac–Coulomb Hamiltonian in Eq. (1.51)]:

$$H = \sum_{i=1}^{N_\mathrm{e}} h(i) + \frac{1}{2} \sum_{i,j\neq i}^{N_\mathrm{e}} g(i,j), \tag{2.6}$$

where $h(i)$ is a one-electron operator, and $g(i,j)$ is a two-electron interaction operator. Let $\chi_a(\boldsymbol{r})$ denote given basis functions constituting a complete basis. Then the occupation number representation of the Hamiltonian is[3]

$$H = h^a{}_b a_a^\dagger a^b + \frac{1}{2} g^{ab}{}_{cd} a_a^\dagger a_b^\dagger a^d a^c, \tag{2.7}$$

[3]Here we do not assume, that the basis is orthonormal (only complete), so we distinguish between covariant and contravariant indices, see Appendix A and the works of Head-Gordon *et al.*[73,74]

where the covariant expressions for h and g are obtained as

$$h_{ab} \equiv \int \chi_a^\dagger(\boldsymbol{r}) h \chi_b(\boldsymbol{r}) d^3\boldsymbol{r} \in \mathbb{C}, \tag{2.8}$$

$$g_{abcd} \equiv \iint \chi_a^\dagger(\boldsymbol{r}_1)\chi_b^\dagger(\boldsymbol{r}_2) g(\boldsymbol{r}_1,\boldsymbol{r}_2)\chi_c(\boldsymbol{r}_1)\chi_d(\boldsymbol{r}_2) d^3\boldsymbol{r}_1 d^3\boldsymbol{r}_2 \in \mathbb{C}. \tag{2.9}$$

h_{ab} and g_{abcd} are called the one- and two-electron integrals, respectively. Here we assumed that the two-electron operator g is independent of electrons' momenta $\boldsymbol{p}_1$ and $\boldsymbol{p}_2$, but no assumption was made for the one-electron part h. $a_a^\dagger$ and a^a are the electron creation and annihilation operators, respectively, satisfying the following anti-commutation relations ($\{\cdot,\cdot\}$ denotes the anti-commutator):

$$\{a^a, a_b^\dagger\} = \delta_b^a, \tag{2.10a}$$

$$\{a^a, a^b\} = 0, \tag{2.10b}$$

$$\{a_a^\dagger, a_b^\dagger\} = 0. \tag{2.10c}$$

In case the Hamiltonian being considered is the Dirac–Coulomb Hamiltonian in Eq. (1.51), the one-electron part h is the 4c matrix in Eq. (1.52), and the basis functions χ_a are 4c column vectors of functions. The two-electron terms g have a trivial multi-component structure. Here, indices a, b, c, d reflect the internal structure of the basis, so that h_{ab} and g_{abcd} are complex *numbers*.[4]

The reduced density matrices can be defined by taking the expectation value of the Hamiltonian in Eq. (2.7). Let $|\Psi\rangle$ denote an orthonormal many-electron state. Then the total energy is

$$E = \langle\Psi|H|\Psi\rangle = h^a{}_b D^b{}_a + \frac{1}{2} g^{ab}{}_{cd} \Gamma^{cd}{}_{ab}, \tag{2.11}$$

where we defined the *one-* and *two-electron reduced density matrix* as

$$D^b{}_a \equiv \langle\Psi|a_a^\dagger a^b|\Psi\rangle\,, \tag{2.12}$$

$$\Gamma^{cd}{}_{ab} \equiv \langle\Psi|a_a^\dagger a_b^\dagger a^d a^c|\Psi\rangle\,, \tag{2.13}$$

[4] Alternatively, it is possible to use the 4×4 matrix form of the basis functions $\chi_\mu(\boldsymbol{r})$ in Eq. (1.29), $h_{\mu\nu}$ is then a 4×4 complex matrix. This distinction is not relevant for what follows in this chapter, so for simplicity the approach based on the scalar h_{ab} elements was chosen.

respectively. These definitions are extended to the time domain in Chapter 3. To simplify our notation, let us introduce traces of the one- and two-electron quantities as

$$\mathrm{Tr}_1\, hD \equiv h^a{}_b D^b{}_a \equiv h_{ab} D^{ba}, \tag{2.14}$$

$$\mathrm{Tr}_2\, g\Gamma \equiv g^{ab}{}_{cd} \Gamma^{cd}{}_{ab} \equiv g_{abcd} \Gamma^{cdab}. \tag{2.15}$$

The total energy then becomes

$$E = \mathrm{Tr}_1\, hD + \frac{1}{2}\,\mathrm{Tr}_2\, g\Gamma. \tag{2.16}$$

2.3 Electron density

Generally, a knowledge of the N-electron density matrix is sufficient to calculate the expectation value of N-electron operators. For instance, for a given one-electron operator A, its expectation value is a simple trace with the one-electron density matrix, *i.e.* $\mathrm{Tr}_1\, AD \equiv A_{ab} D^{ba}$. If a one-electron operator A has a trivial multi-component structure, and contains no derivatives in the coordinate representation, the expectation value $\langle A \rangle$ can be further simplified with the use of the electron density ρ. The relation between the one-electron density matrix and the electron density can be understood from the following analysis. The expectation value of A in the coordinate representation is

$$\langle A \rangle = A_{ab} D^{ba} = \iint d^3\boldsymbol{r}_1 d^3\boldsymbol{r}_2 A_{ss'}(\boldsymbol{r}_1, \boldsymbol{r}_2) D^{s's}(\boldsymbol{r}_2, \boldsymbol{r}_1), \tag{2.17}$$

where s, s' denote four individual bispinor components, and

$$D^{ss'}(\boldsymbol{r}_1, \boldsymbol{r}_2) = \left\langle \Psi \,\middle|\, a^{\dagger s'}(\boldsymbol{r}_2) a^s(\boldsymbol{r}_1) \,\middle|\, \Psi \right\rangle \tag{2.18}$$

is the coordinate representation of the one-electron density matrix. $a^{\dagger s}(\boldsymbol{r})$ and $a^s(\boldsymbol{r})$ are transformed creation and annihilation operators (also known

as the *field operators*), respectively, obtained as[5]

$$a^{\dagger s}(\boldsymbol{r}) = \chi_a^{s*}(\boldsymbol{r}) a^{\dagger a}, \tag{2.19}$$

$$a^{s}(\boldsymbol{r}) = \chi_a^{s}(\boldsymbol{r}) a^{a}. \tag{2.20}$$

Inserting these expression to Eq. (2.18) gives the transformation identity

$$D^{ss'}(\boldsymbol{r}_1, \boldsymbol{r}_2) = \chi_a^s(\boldsymbol{r}_1) D^{ab} \chi_b^{s'*}(\boldsymbol{r}_2). \tag{2.21}$$

Let us assume that A takes the following special form[6]

$$A_{ss'}(\boldsymbol{r}_1, \boldsymbol{r}_2) = \delta(\boldsymbol{r}_1 - \boldsymbol{r}_2) \delta_{ss'} A(\boldsymbol{r}_1), \tag{2.22}$$

where $\delta(\boldsymbol{r})$ is the Dirac delta function. Eq. (2.17) can then be written as

$$\langle A \rangle = \int d^3\boldsymbol{r} A(\boldsymbol{r}) \operatorname{Tr} D(\boldsymbol{r}, \boldsymbol{r}) \equiv \int A(\boldsymbol{r}) \rho(\boldsymbol{r}) d^3\boldsymbol{r}, \tag{2.23}$$

where Tr indicates the trace over the 4 bispinor components, and we defined the 4c spin-less electron density

$$\boxed{\rho(\boldsymbol{r}) \equiv \operatorname{Tr} D(\boldsymbol{r}, \boldsymbol{r})}. \tag{2.24}$$

The electron–nuclear interaction potential is an example of an operator that satisfies Eq. (2.22), and thus can be evaluated as an integral over the electron density. On the other hand, the nonrelativistic kinetic energy operator $(-\frac{\Delta}{2})$ contains the second derivative; its relativistic counterpart $\boldsymbol{\alpha} \cdot \boldsymbol{p}$ is additionally spin-dependent, hence knowledge of the full density matrix may be required.

In practice, the electron density can be evaluated using the given basis functions χ_a. Inserting the transformation identity for the density matrix [Eq. (2.21)] to Eq. (2.24) gives

$$\rho(\boldsymbol{r}) = \operatorname{Tr}\left[\chi_a(\boldsymbol{r}) D^{ab} \chi_b^\dagger(\boldsymbol{r})\right]. \tag{2.25}$$

[5] These relations are consequences of applying the resolution of identity as follows:

$$a^\dagger(\boldsymbol{r}) \left|\mathrm{vac}\right\rangle \equiv \left|\boldsymbol{r}\right\rangle = \sum_a \langle a|\boldsymbol{r}\rangle \left|a\right\rangle \equiv \sum_a \chi_a^*(\boldsymbol{r}) \left|a\right\rangle \equiv \sum_a \chi_a^*(\boldsymbol{r}) a^{\dagger a} \left|\mathrm{vac}\right\rangle,$$

where $|\mathrm{vac}\rangle$ is the vacuum state, and we omitted s for simplicity. Likewise for the annihilation operator.

[6] The trivial multi-component structure is a generalization of the concept of spin-free operators.

If we define the *overlap distribution function* as a product of two basis functions:

$$\Omega_{ab} \equiv \chi_a^\dagger(\boldsymbol{r})\chi_b(\boldsymbol{r}), \tag{2.26}$$

and use the cyclic permutation in Eq. (2.25), we obtain

$$\boxed{\rho(\boldsymbol{r}) = \mathrm{Tr}_1\, \Omega(\boldsymbol{r})D}. \tag{2.27}$$

2.4 SCF equations

2.4.1 Total energy

So far, no approximation has been made, and the expressions for the energy in Eq. (2.16) and the electron density in Eq. (2.27) are exact, given that we know the density matrices. Unfortunately, determining ${D^b}_a$ and ${\Gamma^{cd}}_{ab}$ remains to be the challenging task, and we must resort to approximations. We can make a key observation by assuming, that if $|\Psi\rangle$ corresponds to a single Slater determinant composed of the occupied spinorbitals with indices i, j, k, l, then a straightforward computation gives

$${\tilde{\Gamma}^{ij}}_{kl} = \delta^i_k\delta^j_l - \delta^i_l\delta^j_k, \tag{2.28}$$

and, more generally, in an arbitrary basis:

$${\tilde{\Gamma}^{cd}}_{ab} = {D^c}_a{D^d}_b - {D^c}_b{D^d}_a. \tag{2.29}$$

This motivates us to define the difference two-electron density matrix

$${\bar{\Gamma}^{cd}}_{ab} \equiv {\Gamma^{cd}}_{ab} - {D^c}_a{D^d}_b + {D^c}_b{D^d}_a. \tag{2.30}$$

Substituting this for ${\Gamma^{cd}}_{ab}$ in the energy Eq. (2.16) gives

$$E = \mathrm{Tr}_1\left(h + \frac{1}{2}\left(J[D] - K[D]\right)\right)D + \frac{1}{2}\,\mathrm{Tr}_2\, g\bar{\Gamma}, \tag{2.31}$$

where

$$J_{ab}[D] \equiv g_{acbd}D^{dc}, \tag{2.32}$$
$$K_{ab}[D] \equiv g_{acdb}D^{dc}, \tag{2.33}$$

are the Coulomb (or Hartree) and the exact exchange operators, respectively. Neglecting $\bar{\Gamma}$ yields the well know expression for the HF energy

$$\boxed{E_{\mathrm{HF}} = \mathrm{Tr}_1 \left(h + \frac{1}{2} \left(J[D] - K[D] \right) \right) D}. \tag{2.34}$$

The KS expression for the total energy is similar:

$$\boxed{E_{\mathrm{KS}} = \mathrm{Tr}_1 \left(h + \frac{1}{2} J[D] \right) D + E_{\mathrm{xc}}[\rho]}. \tag{2.35}$$

From a practical point of view, the only difference between the KS and HF energy is that the KS energy does not contain the HF exact exchange operator K, and instead includes the approximate exchange and correlation contributions E_{xc}. Hybrid DFT introduces some portion of K to the KS energy.[71]

In order to establish a connection between the J matrix appearing in the HF and KS energy expressions, and the Coulomb energy in Eq. (2.5), let us insert the two-electron integrals in Eq. (2.9) to Eq. (2.32), set $g(\boldsymbol{r}_1, \boldsymbol{r}_2) \equiv \frac{1}{|\boldsymbol{r}_1 - \boldsymbol{r}_2|}$, and calculate the energy. We obtain

$$E_{\mathrm{H}} \equiv \frac{1}{2} \mathrm{Tr}_1 \, JD = \frac{1}{2} \iint \frac{\mathrm{Tr}_1 \left(\Omega(\boldsymbol{r}_1) D \right) \mathrm{Tr}_1 \left(\Omega(\boldsymbol{r}_2) D \right)}{|\boldsymbol{r}_1 - \boldsymbol{r}_2|} d^3\boldsymbol{r}_1 d^3\boldsymbol{r}_2. \tag{2.36}$$

After realizing that the traces are the electron densities [Eq. (2.27)] we recover Eq. (2.5). Similarly, using Eq. (2.33) we can write the exact exchange energy as

$$E_{\mathrm{x}} \equiv \frac{1}{2} \mathrm{Tr}_1 \, KD = \frac{1}{2} \iint \frac{\mathrm{Tr}_1 \left(\Omega(\boldsymbol{r}_1) D \Omega(\boldsymbol{r}_2) D \right)}{|\boldsymbol{r}_1 - \boldsymbol{r}_2|} d^3\boldsymbol{r}_1 d^3\boldsymbol{r}_2. \tag{2.37}$$

We note that these expressions for the Coulomb and exact exchange energy are general, and can be used both in the 1c, 2c, and 4c frameworks. The product of the two traces in the Coulomb energy makes its implementation much simpler compared to the exact exchange energy, which cannot be factorized, and usually requires more operations to compute. For the hybrid-type functionals, the E_{xc} term is approximated as

$$E_{\mathrm{xc}} = \int \varepsilon_{\mathrm{xc}}[\rho, \boldsymbol{\nabla}\rho, \xi](\boldsymbol{r}) d^3\boldsymbol{r} + \xi E_{\mathrm{x}}, \tag{2.38}$$

where ξ is a weight factor for the HF exchange contribution, and $\varepsilon_{\mathrm{xc}}$ is a function of the density and its gradient; the factor ξ multiplies the exchange part of $\varepsilon_{\mathrm{xc}}$.

2.4.2 One-electron equations

The HF and KS energy require knowledge of the one-electron density matrix. Once D is determined, the electron density needed for the E_{xc} term can be constructed from Eq. (2.27). Within the HF and KS framework the one-electron density matrix is composed *approximately*, *i.e.* from the solutions of the effective self-consistent one-electron equations.[7] These equations can be derived by applying the variational principle,[36,63,64] and take the form

$$F\varphi_p(\boldsymbol{r}) = \varepsilon_p \varphi_p(\boldsymbol{r}), \tag{2.39}$$

where F is the Fock operator, φ_p are the molecular orbitals (MOs) and ε_p are the orbital energies. Expanding the MOs as

$$\varphi_p(\boldsymbol{r}) = \chi_a(\boldsymbol{r}) c^a{}_p, \tag{2.40}$$

where $c^a{}_p$ are the MO expansion coefficients, gives the matrix form of Eq. (2.39)

$$\boxed{Fc = Sc\varepsilon}. \tag{2.41}$$

Here, ε labels the diagonal matrix of spinorbital energies,

$$S_{ab} = \int \chi_a^\dagger(\boldsymbol{r}) \chi_b(\boldsymbol{r}) d^3\boldsymbol{r} \tag{2.42}$$

is the *overlap matrix*, and the Fock matrix F is obtained as the energy derivative

$$F_{ab} = \frac{\partial E}{\partial D^{ba}}. \tag{2.43}$$

Evaluating the derivative gives

$$\boxed{F = h + J - \xi K + V^{\text{xc}}}, \tag{2.44}$$

where $(\varepsilon_{\text{xc}}[\rho, \boldsymbol{\nabla}\rho, \xi] \equiv \varepsilon_{\text{xc}})$

$$J_{ab}[D] = \iint \frac{\Omega_{ab}(\boldsymbol{r}_1)\, \text{Tr}_1\left(\Omega(\boldsymbol{r}_2) D\right)}{|\boldsymbol{r}_1 - \boldsymbol{r}_2|} d^3\boldsymbol{r}_1 d^3\boldsymbol{r}_2, \tag{2.45a}$$

$$K_{ab}[D] = \iint \frac{\left(\Omega(\boldsymbol{r}_1) D \Omega(\boldsymbol{r}_2)\right)_{ab}}{|\boldsymbol{r}_1 - \boldsymbol{r}_2|} d^3\boldsymbol{r}_1 d^3\boldsymbol{r}_2, \tag{2.45b}$$

$$V^{\text{xc}}_{ab}[\rho, \boldsymbol{\nabla}\rho, \xi] = \int \frac{\partial \varepsilon_{\text{xc}}}{\partial \rho(\boldsymbol{r})} \Omega_{ab}(\boldsymbol{r}) + \frac{\partial \varepsilon_{\text{xc}}}{\partial \boldsymbol{\nabla}\rho(\boldsymbol{r})} \cdot \boldsymbol{\nabla}\Omega_{ab}(\boldsymbol{r}) d^3\boldsymbol{r}. \tag{2.45c}$$

[7] Such a density matrix corresponds to a state described by a single Slater determinant, compared to the exact density matrix which corresponds to the true wave function.

The expressions for J and K are identical to those in Eqs. (2.32) and (2.33). The Fock matrix in Eq. (2.44) corresponds to hybrid DFT, however, setting $\xi = 1$ (for which $V^{\mathrm{xc}} = 0$) yields the HF method, and setting $\xi = 0$ one recovers pure KS DFT.

The density matrix expressed in the basis of MOs is the diagonal occupation matrix f, containing ones and zeros for the occupied and vacant spinorbitals, respectively. MOs corresponding to the negative-energy states are left vacant. The AO density matrix is obtained by transforming f as

$$D = cfc^{\dagger}. \tag{2.46}$$

The SCF Eq. (2.41) is nonlinear (self-consistent), due to the dependence of the Fock matrix on the the density matrix which is determined from the coefficients c. Therefore, Eq. (2.41) must be solved iteratively. The convergence of the SCF procedure was dramatically improved by Pulay[75,76] who introduced the direct inversion of the iterative subspace (DIIS) scheme. DIIS involves construction of an error vector evaluated as the commutator $[F, D]$ in each cycle. The error vectors from the current and the previous cycles then enter a minimization procedure that yields a set of coefficients used to extrapolate the Fock matrix.

2.5 Gaussian-type functions

In this section we briefly discuss the fundamental build units of the SCF method used in this work, *i.e.* atom-centered normalized primitive Cartesian Gaussian-type orbitals (GTOs).[77,78] Cartesian GTOs are defined as

$$g_{\mu}(\boldsymbol{r}) \equiv \mathcal{N}(x - A_x)^{l_x}(y - A_y)^{l_y}(z - A_z)^{l_z} e^{-\alpha(\boldsymbol{r}-\boldsymbol{A})^2}, \tag{2.47}$$

where $\mathcal{N}$ is the normalization constant, $\boldsymbol{\alpha}$ is the Gaussian exponent, $\boldsymbol{l} \equiv (l_x, l_y, l_z)$ are the Cartesian angular momenta, and $\boldsymbol{A}$ and $\boldsymbol{r}$ are the nuclear and electron coordinates, respectively. In most cases, integrals containing GTOs can be evaluated analytically using various recurrence relations.[63,78] GTOs g_{μ} constitute a set of scalar 1c basis functions; the 4c basis is constructed by employing Eqs. (1.29) and (1.30) to respect the RKB condition (see Section 1.2).

One of the major advantages of the GTO basis is that matrix elements of many operators expressed in this basis decay rapidly with an increasing

separation of the Gaussian centers. This is a consequence of the Gaussian product rule:[63]

$$e^{-\alpha(\boldsymbol{r}-\boldsymbol{A})^2}e^{-\beta(\boldsymbol{r}-\boldsymbol{B})^2} = e^{-\mu(\boldsymbol{B}-\boldsymbol{A})^2}e^{-p(\boldsymbol{r}-\boldsymbol{P})^2}, \tag{2.48}$$

where we defined

$$\mu \equiv \frac{\alpha\beta}{\alpha+\beta}, \qquad p \equiv \alpha+\beta, \qquad \boldsymbol{P} \equiv \frac{\alpha\boldsymbol{A}+\beta\boldsymbol{B}}{\alpha+\beta}. \tag{2.49}$$

Here we can see that the factor $e^{-\mu(\boldsymbol{B}-\boldsymbol{A})^2}$ in the product ensures the exponential decay as the distance between $\boldsymbol{A}$ and $\boldsymbol{B}$ increases.

The computationally most expensive part of the SCF algorithm is the evaluation of the two-electron integrals in Eq. (2.9), and their subsequent contraction with the density matrix in Eqs. (2.45a) and (2.45b). Due to the incredibly large number of the two-electron integrals in solid-state calculations in **Paper V**, these integrals are approximated using the spherical multipole expansion.[63] This approximation requires making the extent of the Gaussian products finite. We define the extent of the Gaussian product r_p as[79,80]

$$r_p \equiv p^{-1/2}\,\mathrm{erfc}^{-1}\,\varepsilon, \tag{2.50}$$

where ε is a small positive threshold, and

$$\mathrm{erfc}(x) \equiv \frac{2}{\sqrt{\pi}}\int_x^\infty e^{-t^2}dt \tag{2.51}$$

is the complementary error function. This definition ensures that integrating a normalized Gaussian over the region beyond its extent gives a negligible contribution

$$2\sqrt{\frac{p}{\pi}}\int_{r_p}^\infty e^{-px^2}dx = \varepsilon. \tag{2.52}$$

Chapter 3

Real-time electron dynamics

> Big things have small beginnings.
>
> *David* in Prometheus

This chapter introduces the main principles that are further developed and applied in **Paper I**–**IV** in the study of the response of molecules to external time-dependent fields. Perturbing the ground state of a molecule with a time-dependent electric or magnetic field causes the system to enter a state that is a superposition of all excited states. Propagating this state in time enables probing various spectroscopic properties, such as valence absorption spectroscopy [**Paper I**], core electron (X-ray) spectroscopy [**Paper II**], electronic circular dichroism (ECD) and optical rotatory dispersion (ORD) [**Paper IV**], and nonlinear optical processes [**Paper III**]. Relativity plays an important role in many of these properties, since it affects the structure of orbitals – scalar relativity induces shifts in orbital energies, and the SOC additionally splits the otherwise degenerate orbital energies. Hence the excited states that involve excitations to and from such orbitals are qualitatively differently described at the nonrelativistic and relativistic levels of theory. This is particularly true for core-lying orbitals, where the relativistic effects are known to be most prominent, and can be observed also for light elements of the periodic table.

So far we have only considered the electronic ground state, and the *static* SCF method described in Chapter 2 was designed to yield the approximate ground state energy and the optimized HF or KS orbitals and their corre-

sponding energies. In this chapter we extend the previous SCF formalism by including an explicit time-dependence to the one-electron Hamiltonian to account for the time-dependence of the external fields. The time evolution of the system characterized by this Hamiltonain can be approximately described by the time-dependent SCF (TDSCF) equation, which is a time-dependent analogue of the static SCF. We solve this equation directly in the time domain, and propagate the one-electron time-dependent density matrix. This is in contrast with the more common perturbative approach, where the linear response theory is developed,[81–84] and equations in the frequency domain are formulated.[85,86] The differences between the two approaches will also be discussed here. When the TDSCF equation is solved in the time domain, this method is sometimes referred to as *real-time* TDSCF to distinguish it from the perturbative frequency-domain based methods.

3.1 Liouville–von Neumann equation

3.1.1 Time-dependent Hartree–Fock

The time-dependent analogue of the HF equation can be derived by applying similar arguments as for its static counterpart (see Section 2.1). Approximating the many-electron wave function at each time t with a single Slater determinant, and employing the time-dependent variational principle yields a set of nonlinear equations for the *time-dependent* spinorbitals[36,87–89] – their time evolution is governed by the time-dependent Fock operator. These equations can be recast into the Liouville–von Neumann (LvN) equation for the one-electron density matrix.

Here, we pursue an alternative path to the LvN equation at the HF level.[90] We first derive an exact equation for the time evolution of the one-electron density matrix, then introduce the HF approximation to obtain the LvN equation. Let

$$H(t) = h^a{}_b(t) a_a^\dagger a^b + \frac{1}{2} g^{ab}{}_{cd} a_a^\dagger a_b^\dagger a^d a^c \tag{3.1}$$

be an explicitly time-dependent Hamiltonian, where

$$h_{ab}(t) \equiv \int \chi_a^\dagger(\boldsymbol{r}) h(t) \chi_b(\boldsymbol{r}) d^3\boldsymbol{r} \in \mathbb{C}, \tag{3.2}$$

$$g_{abcd} \equiv \iint \chi_a^\dagger(\boldsymbol{r}_1) \chi_b^\dagger(\boldsymbol{r}_2) g(\boldsymbol{r}_1, \boldsymbol{r}_2) \chi_c(\boldsymbol{r}_1) \chi_d(\boldsymbol{r}_2) d^3\boldsymbol{r}_1 d^3\boldsymbol{r}_2 \in \mathbb{C}. \tag{3.3}$$

Here, the interaction of electrons with an external time-dependent field is incorporated in the one-electron Hamiltonain $h(t)$. Furthermore, let $|\Psi(t)\rangle$ denote the orthonormal time-dependent many-electron state satisfying

$$i\frac{\partial}{\partial t}\,|\Psi(t)\rangle = H(t)\,|\Psi(t)\rangle\,. \tag{3.4}$$

The definitions of the density matrices in Eqs. (2.12) and (2.13) can straightforwardly be extended to the time domain as

$$D^{b}{}_{a}(t) \equiv \langle\Psi(t)|a_a^\dagger a^b|\Psi(t)\rangle\,, \tag{3.5}$$

$$\Gamma^{cd}{}_{ab}(t) \equiv \langle\Psi(t)|a_a^\dagger a_b^\dagger a^d a^c|\Psi(t)\rangle\,. \tag{3.6}$$

Taking the time derivative of Eq. (3.5), and applying Eq. (3.4) gives

$$i\frac{\partial}{\partial t}D^{b}{}_{a}(t) = -\left\langle\Psi(t)\,\middle|\,\left[H(t), a_a^\dagger a^b\right]\,\middle|\,\Psi(t)\right\rangle. \tag{3.7}$$

The commutator in this equation can be evaluated utilizing algebraic rules for commutators and anti-commutators together with Eqs. (2.10). It follows, that Eq. (3.7) can be written as

$$\boxed{i\frac{\partial}{\partial t}D(t) = [h(t), D(t)] + \frac{1}{2}\,\mathrm{Tr}_1\,[\tilde{g}, \Gamma(t)]}, \tag{3.8}$$

where we defined the following shorthand notation:

$$\tilde{g}^{ab}{}_{cd} \equiv g^{ab}{}_{cd} - g^{ab}{}_{dc}, \tag{3.9a}$$

$$(g\Gamma)^{ab}{}_{cd} \equiv g^{ab}{}_{ef}\Gamma^{ef}{}_{cd}, \tag{3.9b}$$

$$(\mathrm{Tr}_1\,X)^{a}{}_{b} \equiv X^{ac}{}_{bc}, \tag{3.9c}$$

for any two-electron operator X. Eq. (3.8) is an exact equation determining the time evolution of the one-electron density matrix. Unfortunately, this equation cannot be solved, because the two-electron density matrix $\Gamma(t)$ is not known. Hence we could follow a similar procedure that we used to obtain Eq. (3.8) to derive a similar time-dependent equation for $\Gamma(t)$. However, this equation would then contain the undetermined three-electron density matrix. Continuing this process for the three-, four-,... electron density matrices would yield a system of linear differential equations for the density matrices that is essentially equivalent to the time-dependent Schrödinger

equation for the many-electron equation. This system of equations can easily be decoupled by introducing the HF approximation (see Section 2.4)

$$\Gamma^{cd}{}_{ab}(t) \approx D^{c}{}_{a}(t)D^{d}{}_{b}(t) - D^{c}{}_{b}(t)D^{d}{}_{a}(t) \tag{3.10}$$

in Eq. (3.8). We obtain the time-dependent HF equation

$$iS\left[\frac{\partial}{\partial t}D(t)\right]S = F(t)D(t)S - SD(t)F(t), \tag{3.11}$$

where $F(t)$ is the time dependent Fock matrix

$$F(t) = h(t) + J[D(t)] - K[D(t)], \tag{3.12}$$

J and K are defined in Eqs. (2.32) and (2.33). We introduced the overlap matrix S [Eq. (2.42)] so that we adhere to the commonly used notation where the Fock matrix elements transform covariantly as F_{ab}, and the density matrix elements transform contravariantly as D^{ab} (see Appendix A). In an orthonormal basis ($S = \mathbb{I}$) Eq. (3.11) becomes

$$\boxed{i\frac{\partial}{\partial t}D(t) = [F(t), D(t)]}. \tag{3.13}$$

This equation is sometimes referred to as the Liouville–von Neumann equation or the TDSCF equation, and plays the central role in **Paper I–IV**. Note, that due to the dependence of the Fock matrix on the density matrix, this is a nonlinear equation.

3.1.2 Time-dependent density functional theory

Developing the time-dependent equivalent of the KS DFT requires deeper considerations.[87] The Runge–Gross theorem establishes a mapping between the time-dependent electron density and an external potential[91] — the time-dependent generalization of the Hohenberg–Kohn theorem. Van Leeuwen's theorem then connects two systems with two different interaction potentials.[92] Choosing one of the systems to be a fictitious non-interacting system substantiates the use of the time-dependent variant of the KS method. The resulting equation is the same as Eq. (3.13) except that the Fock matrix is given as

$$F(t) = h(t) + J[D(t)] - \xi K[D(t)] + V^{\mathrm{xc}}[\rho(t), \boldsymbol{\nabla}\rho(t), \xi], \tag{3.14}$$

where ξ is a weight of the exact exchange term ($\xi = 0$ for pure DFT functional), and V^{xc} is given by Eq. (2.45c).

3.2 Evolution operator

Various time propagation schemes for the Schrödinger[93] and the LvN equation have been studied.[94–98] To formulate a solution of Eq. (3.13) directly in time domain, it is convenient to define the *evolution operator* (matrix) U as a unitary transformation

$$D(t) = U(t,t')D(t')U^{\dagger}U(t,t'). \tag{3.15}$$

Given that we know the density matrix at time t', the evolution operator allows us to express D in an arbitrary time t. It is easy to show the following properties of U:

$$U(t,t) = \mathbb{I}, \tag{3.16a}$$
$$U(t_3,t_1) = U(t_3,t_2)U(t_2,t_1), \tag{3.16b}$$
$$U^{\dagger}(t_1,t_2) = U(t_2,t_1). \tag{3.16c}$$

3.2.1 Dyson series

To determine U we insert Eq. (3.15) into the LvN Eq. (3.13). It follows that

$$\left(i\dot{U} - FU\right)DU^{\dagger} - UD\left(i\dot{U} - FU\right)^{\dagger} = 0, \tag{3.17}$$

where $U \equiv U(t,t')$, $D \equiv D(t')$, and the dot denotes the time derivative. Carefully considering the free parameters of U, and projection properties of D, it can be show that it is sufficient to satisfy

$$i\dot{U}(t,t') = F(t)U(t,t'). \tag{3.18}$$

This differential equation for U can be transformed to the integral form

$$U(t,t') = \mathbb{I} - i\int_{t'}^{t} F(\tau)U(\tau,t')d\tau. \tag{3.19}$$

Replacing $U \to U_k$ on the right-hand side, and $U \to U_{k+1}$ on the left-hand side of this equation, and solving the so-obtained recurrence relation, yields the evolution operator in the form of the *Dyson series*:

$$U(t,t') = \sum_{n=0}^{\infty}\frac{(-i)^n}{n!}\int_{t'}^{t}dt_1\ldots\int_{t'}^{t}dt_n T\{F(t_1)\ldots F(t_n)\}, \tag{3.20}$$

or, in a shorthand notation:

$$U(t,t') = T\exp\left[-i\int_{t'}^{t} F(\tau)d\tau\right]. \tag{3.21}$$

Here, T designates that the product of Fock matrices is *time-ordered*.[1] Terms in the time-ordered product are sorted from the left to right in a descending order of their corresponding value of t, *i.e.* the term with the highest value of time is the first on the left. This time-ordering accounts for the fact that the Fock matrices expressed at different times do not generally commute. If the Fock matrix is time-independent ($F(t) \equiv F_0$), Eq. (3.21) simplifies to

$$U_0(t,t') = e^{-iF_0(t-t')}. \tag{3.22}$$

3.2.2 Magnus expansion

A numerical evaluation of the Dyson series in Eq. (3.20) is cumbersome due to the time-ordering operator T. Expanding and truncating the series to approximate the evolution operator will break essential properties of the time propagation, such as the idempotency of the density matrix, and this can cause various numerical instabilities in the implementation.[94,95,97] To mitigate these issues Magnus proposed an alternative form of the expansion.[99] This expansion is known as the *Magnus expansion* and takes the form of

$$U(t,t') = e^{A(t,t')}, \tag{3.23}$$

where

$$A(t,t') = \sum_{n=1}^{\infty} A_n(t,t'), \tag{3.24}$$

and the first three terms are given as[88,99]

$$A_1(t,t') = -i\int_{t'}^{t} dt_1 F(t_1), \tag{3.25a}$$

$$A_2(t,t') = -\frac{1}{2}(-i)^2\int_{t'}^{t} dt_2\int_{t'}^{t_2} dt_1\big[F(t_1),F(t_2)\big], \tag{3.25b}$$

$$\begin{aligned} A_3(t,t') = &-\frac{1}{6}(-i)^3\int_{t'}^{t} dt_3\int_{t'}^{t_3} dt_2\int_{t'}^{t_2} dt_1\Big[F(t_1),\big[F(t_2),F(t_3)\big]\Big] \\ &+\Big[\big[F(t_1),F(t_2)\big],F(t_3)\Big]. \end{aligned} \tag{3.25c}$$

[1] See Tannor[88], for example.

When the series in Eq. (3.24) is truncated after any number of terms, the evolution operator will remain to be *exactly* unitary, which will preserve the properties of the density matrix.

3.3 Perturbation operator

The interaction of a studied system with an external field enters the Hamiltonian via its one-electron part $h(t) \equiv h + h'(t)$, where h is the time-independent part describing the system itself (*e.g.* the Dirac Hamiltonain in Eq. (1.24)), and $h'(t)$ contains the interaction with external fields. As a consequence, the time-dependent Fock matrix in Eq. (3.14) can be written as

$$F(t) \equiv F[D(t), t] = F_0[D(t)] + V^{\text{ext}}(t), \tag{3.26}$$

where $F_0[D(t)]$ contains the terms that *implicitly* depend on time via the density matrix and the electron density:

$$F_0[D(t)] \equiv h + J[D(t)] - \xi K[D(t)] + V^{\text{xc}}[\rho(t), \boldsymbol{\nabla}\rho(t), \xi], \tag{3.27}$$

and $V^{\text{ext}}(t)$ is the explicitly time-dependent part. In **Paper I**, **II**, and **IV** $V^{\text{ext}}(t)$ is chosen to take the form of a homogeneous electric field with a delta-function time dependence, *i.e.*

$$V^{\text{ext}}(t) = -\boldsymbol{\kappa}\delta(t) \cdot \boldsymbol{\mu}, \tag{3.28}$$

where $\boldsymbol{\mu} \equiv -\boldsymbol{r}$ is the electron dipole moment operator, and $\boldsymbol{\kappa}$ represents the strength and the orientation of the electric field. Generally, $V^{\text{ext}}(t)$ can have the form of

$$V^{\text{ext}}(t) = \kappa(t)P(t), \tag{3.29}$$

where $\kappa(t)$ is a "small" time-dependent amplitude of the perturbation, and $P(t)$ is a one-electron operator, very often time-independent.[2] Finally, in response theory[83,85,86] V^{ext} is a periodic function modulated by a factor $e^{\gamma t}$ to account for the perturbation that is *slowly* switched on, $\gamma > 0$ is a small real number. Specifically

$$V^{\text{ext}}(t) = \sum_k \kappa_k P_k e^{-i\omega_k t + \gamma t}. \tag{3.30}$$

[2]The purpose of the factorization of V^{ext} to the amplitude and the operator part is that one can later construct a perturbation expansion, given that the amplitude is small.

Here, k runs over a finite list of chosen frequencies ω_k, P_k is the one-electron operator associated with this frequency, and κ_k is its amplitude.[3]

3.4 Real-time propagation vs. response theory

Solutions to Eq. (3.13) can be sought in the form of the perturbation expansion

$$\begin{aligned} D(t) =& D^{(0)} + \int_{-\infty}^{t} dt_1 D^{(1)}(t-t_1)\kappa(t_1) + \\ &+ \frac{1}{2!}\int_{-\infty}^{t} dt_1 \int_{-\infty}^{t} dt_2 D^{(2)}(t-t_1, t-t_2)\kappa(t_1)\kappa(t_2) + \ldots, \end{aligned} \tag{3.31}$$

where $\kappa(t)$ is the time-dependent amplitude of the external field, and $D^{(i)}$ are the perturbed density matrices. For $\kappa(t) = \sum_k \kappa_k e^{-i\omega_k t+\gamma t}$ (see Eq. (3.30)) we obtain the equivalent expansion of the time-dependent density matrix in the frequency domain[83,85]

$$\begin{aligned} D(t) =& D^{(0)} + \sum_k \kappa_k D^{(1)}(\omega_k) e^{-i\omega_k t+\gamma t} \\ &+ \frac{1}{2!}\sum_{kk'} \kappa_k \kappa_{k'} D^{(2)}(\omega_k, \omega'_k) e^{-i(\omega_k+\omega_{k'})t+2\gamma t} + \ldots. \end{aligned} \tag{3.32}$$

If $D^{(0)} \equiv D_0$ is the ground-state density matrix obtained from the time-independent SCF, and we insert this expansion into the LvN Eq. (3.13), neglecting the quadratic $D^{(2)}$ and higher terms, yields the linear response equation.[84] Due to the dependence of several terms in Eq. (3.27) on the density matrix (or density), the response kernels originating from $\frac{\partial F_{ab}[D]}{\partial D^{cd}}$ enter the response equation, and complicate the implementation of its solution.[100]

The approach based on the propagation of the density matrix in real time has several advantages over the response theory. Direct solution of the LvN equation only requires constructing the Fock matrix at each time step, and thus avoids the evaluation of the response kernels $\frac{\partial F_{ab}[D]}{\partial D^{cd}}$ that enter the linear response equation. Therefore, implementation of the real-time method can use the same Fock-assembling routines as the SCF procedure, and any acceleration techniques that enhance the Fock matrix construction

[3] To be precise, the list of k contains pairs of frequencies ω_k and $\omega_{-k} \equiv -\omega_k$ for each k, and $\kappa_{-k} = \kappa_k^*$ and $P_{-k} = P^\dagger$ must be satisfied so that V^{ext} is Hermitian.

are directly transferred to the TDSCF. The non-perturbational nature of the method enables extraction of nonlinear optical properties, as demonstrated in **Paper III**. TDSCF is well-suited for simulating electron dynamics in strong fields, fast processes, and molecular dynamics. In addition, using the δ-type pulse to perturb a system simultaneously awakens all its excited states, and one real-time simulation run can yield spectra in a large energy window.

The real-time propagation method has some disadvantages. TDSCF requires the development of a stable and robust time propagator – this task is not straightforward even when the Magnus expansion Eq. (3.23) is employed because of the implicit dependence of the unperturbed Fock matrix on time (via the density matrix). From the computational perspective the real-time method has a large prefactor, and may require long simulations with many Fock matrix constructions, if spectra at high resolution are desired. Finally, it is unclear how to identify the origin of individual excitations from the real-time simulation. These issues will be addressed in the next section. More information about the recent progress in real-time methods can be found in the review of Goings, Lestrange and Li.[101]

3.5 Summary of contributions

I conclude this chapter by providing a summary of the main advancements and results presented in **Paper I**–**IV**. These publications involve extending the relativistic 4c and 2c methods to the time domain, solving the LvN Eq. (3.13) with the 4c Dirac Hamiltonian by propagating the one-electron density matrix in real time. We apply this formalism to probe various properties and spectroscopies.

3.5.1 Paper I

In this work we presented the first implementation of the 4c real-time TDSCF. Initial versions of the solver that propagates the density matrix based on the Magnus expansion Eq. (3.23) proved to be unstable, and we experienced catastrophic behavior after some propagation time. After several tests we identified that the solver was not reflecting the nonlinear nature of the LvN equation sufficiently, this was particularly true at the DFT level,

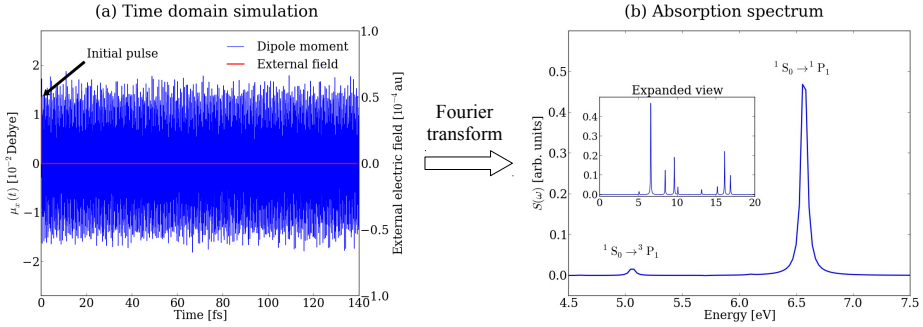

Figure 3.1. Time development of the induced dipole moment and the absorption spectrum of the mercury atom obtained from the real-time propagation after applying the delta-type pulse. We observed the singlet–triplet transition (the first peak from the left) that is forbidden in the nonrelativistic theory.

i.e. when the XC contributions were included. The Magnus expansion was originally designed to solve linear differential equations, and to tackle the nonlinear terms [see Eq. (3.27)] in the LvN equation, additional improvements to the propagation method are required to reach self-consistent solutions. We tested various solvers, and introducing an extrapolation and interpolation scheme[98] stabilized the time propagation. The details of this method can be found in **Paper I**.

To obtain the absorption spectra, we first perturb the ground state of a studied system with a delta-type pulse in Eq. (3.28). The propagated density matrix is then used to calculate the induced dipole moment $\boldsymbol{\mu}(t)$ at each time step. The absorption spectrum is constructed as the Fourier transform of the dynamic polarizability that is obtained from the induced dipole moments. Fig. 3.1 illustrates this process for the mercury atom. We assessed the real-time method by comparing our results for the excitation energies with the available relativistic linear-response time-dependent DFT results as well as with experimental data.

To facilitate the identification of the excitations, we introduced the dipole-weighted transition matrix analysis. The analysis is performed in the basis of the ground-state MOs, and relies on examining partial contributions of the occupied–virtual spinorbital pair ai to the polarizability $\alpha(t)$,

i.e.

$$\alpha_{\boldsymbol{n},ai}(t) = \frac{1}{\kappa}\left[P_{\boldsymbol{n},ia}D_{ai}(t) + P_{\boldsymbol{n},ai}D_{ia}(t)\right], \tag{3.33}$$

where $\boldsymbol{n}$ denotes the orientation of the external electric field, kappa is the field strength, and $P_{\boldsymbol{n}}$ is the electric dipole moment matrix. This decomposition was later used by Bruner *et al.*[102] to accelerate the real-time method by reducing the required simulation lengths.

Since the perturbation operator is proportional to the Dirac delta function, the initial perturbation can be performed analytically for the Fock operator

$$F(t) = F_0[D(t)] + P\delta(t), \tag{3.34}$$

where P is an arbitrary one-electron operator. Then the perturbed density matrix at $t = 0^+$ is expressed as

$$D(0^+) = e^{-iP}D_0e^{iP}. \tag{3.35}$$

The proof of this statement in the TDSCF framework requires a careful consideration of the nonlinear terms in the LvN equation, and is shown in the Appendix of **Paper I**.

3.5.2 Paper II

Here, the method outlined in **Paper I** is applied to obtain the X-ray photoabsorption cross section of the SF_6 molecule near $L_{2,3}$-edges of the sulfur atom. The studied region of the spectrum is dominated by the excitation from the core sulfur p orbitals. Located in the close vicinity of the nucleus, core electron orbitals are most significantly affected by the relativistic effects. The three core p orbitals are split to two $p_{3/2}$ and one $p_{1/2}$ orbitals due to the spin–orbit coupling, giving rise to the $L_{2,3}$-edge resonances in the photoabsorption spectrum. We performed both relativistic and nonrelativistic calculations to demonstrate this effect.

We used the transition analysis developed in **Paper I** to assign the irreducible representations of the octahedral point group (a_{1g}, t_{2g}, and e_g) to the individual resonances. Fig. 3.2 depicts the result of this analysis for the first four most dominant resonances. The number of active virtual spinorbitals helped us determine the irreducible representation of the transition.

The initial absorption spectrum contained many resonances of unclear origin in the sulfur L-edge region. Our transition analysis of those peaks

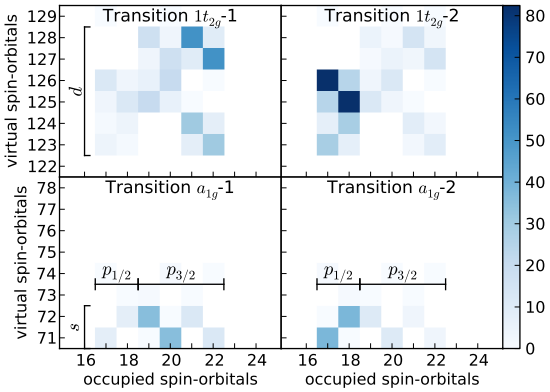

Figure 3.2. The dipole transition analysis of the first four dominant transitions in the X-ray absorption spectrum. More intense excitations are shown with the more intense blue color. The numbers 17–22 on the x-axis label the six sulfur p spinorbitals, the numbers on the y-axis label virtual spinorbitals, where 71 is the first unoccupied spinorbital.

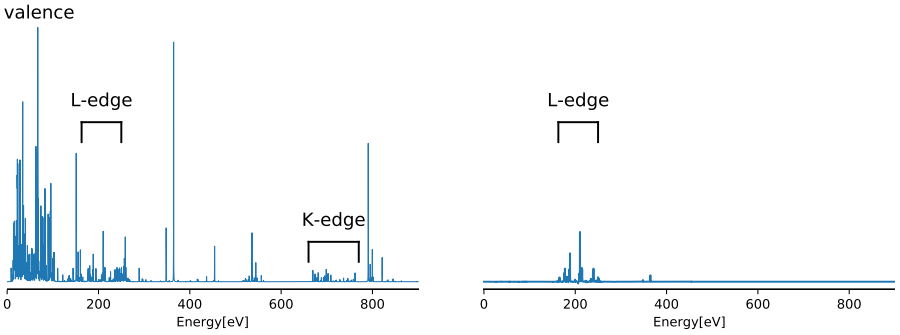

Figure 3.3. Photoabsorption spectra of the SF_6 molecule from a simulation using the full perturbation operator (left) and the restricted perturbation operator (right).

revealed that they emerged from excitations from the valence states to nonphysical high-lying virtual orbitals. Such intruder states are merely artifacts of calculations that employ finite bases, and hinder the interpretation of results. Therefore, we restricted the perturbation operator only to excitations from the sulfur 2p spinorbital, zeroing all matrix elements that correspond to nonphysical or unwanted excitations. Fig. 3.3 shows a com-

parison between the spectrum obtained from a calculation with the full and restricted perturbation operator, respectively. Note, that the restriction is only applied to the perturbation operator, retaining the relaxation of all spinorbitals during the time propagation.

3.5.3 Paper III

In this work we introduced the X2C transformation (see Section 1.5) to the 4c LvN equation to eliminate the positronic states. The main motivation was to accelerate the time propagation, and to asses the X2C transformation for the TDSCF equation. The results obtained at the 2c level of theory agree perfectly with the reference 4c results. In addition, a speedup of 7 or more was achieved by the X2C transformation. Hence, we demonstrated that the relativistic real-time simulations are possible at a reduced price without the loss of accuracy.

In time domain, the X2C decoupling matrix U is time-dependent, and the X2C transformed LvN equation contains the term $\propto \partial U(t)/\partial t$. However, we argue that the error from neglecting this term is of the same order of magnitude as the error arising from the dipole approximation. Therefore, the time-dependence of the decoupling matrix can safely be ignored within the dipole approximation.

We exploit the nonperturbative nature of the real-time method to study nonlinear optical properties, *i.e.* polarizability, first and second hyperpolarizability tensors. We obtain these properties in the frequency domain by performing several simulations in the time domain with harmonic perturbations. The (hyper)polarizabilities are extracted by identifying corresponding terms in the perturbative expansion of the induced dipole moment.

3.5.4 Paper IV

Here, we extended the relativistic real-time solver to incorporate the magnetic dipole operator needed to study ECD and ORD spectra of chiral molecules of the dimethylchalcogenirane series. The necessity to calculate the chiroptical properties of these molecules at the relativistic level becomes apparent for Po and Lv, but differences can already be observed for Se and Te. In addition, the nonrelativistic ECD spectrum of Po is a mirror image of its relativistic counterpart in a certain frequency region, hence interpreting

the spectrum while ignoring the relativistic effects could yield qualitatively incorrect conclusions.

From the methodological perspective further accelerations are introduced here to facilitate the real-time simulations of electron dynamics of larger molecules. Both the X2C transformation and the resolution-of-identity approximation for the Coulomb term (density fitting) is formulated for the first time in complex quaternion algebra. Both approximations introduce only negligible errors, as we demonstrate by comparing the results obtained at various approximation setups. Moreover, by introducing these approximations the simulations are accelerated by a factor of almost 25 compared to the more exact calculations, making the real-time propagation method a competitive tool for studying electron dynamics subjected to external fields.

Chapter 4

Periodic systems

> He who fights with monsters might take care lest he thereby become a monster. And if you gaze for long into an abyss, the abyss gazes also into you.
>
> *Friedrich Nietzsche*

Modeling materials in the solid state from first principles poses a formidable challenge to available quantum-mechanical methods. This fact is even more pronounced for relativistic methods, where conventional approaches based on plane waves can suffer serious deficiencies. Most quantum-chemical methods can straightforwardly be extended from molecules to solids or periodic systems,[1] at least in principle. In practice, new challenges arise at almost every level of reasoning. While it is not immediately obvious why the transition from finite to periodic systems introduces complications, deeper analysis reveals that the infinite aspect of the systems must be considered across multiple domains of algorithms. In view of this observation, Fulde questions whether the approaches based on controlled and systematic approximations as used in quantum chemistry can be realized in solid-state theory as well.[103] Despite the fact that the vast majority of solid-state calculations are performed at the DFT level as is today also the case for molecules, approximations that simplify and accelerate

[1] "Periodic systems" is a common name used for systems that periodically extend to infinity in one, two or three spatial dimensions.

the computation must be employed to a degree that the reproducibility of results across various approximation schemes can questioned. [104]

Developing the relativistic 4c SCF method was the major part of my PhD work, and this chapter constitutes an introduction to the topic; **Paper V** outlines the theory and the method in greater detail. Formally, I only introduce a few extra principles besides the ones presented in Chapter 2.

4.1 Translational invariance

4.1.1 Bravais lattice

A periodic system is constructed by periodically replicating a motif (*unit cell*) in d periodic dimensions, where $d = 1, 2, 3$. In our case, the unit cell can be an atom, a molecule or even a set of molecules. The pattern according to which the unit cell is replicated is given by the d primitive lattice vectors $\boldsymbol{a}_i$ for $i = 1, \ldots, d$. Then each unit cell position vector $\boldsymbol{m}$ can be written as

$$\boldsymbol{m} = m^i \boldsymbol{a}_i, \qquad m^i \in \mathbb{Z}, i = 1, \ldots, d. \tag{4.1}$$

Fig. 4.1 shows and example of a two-dimensional hexagonal Bravais lattice with two atoms in a unit cell. The unit cell $\boldsymbol{m} = \boldsymbol{0}$ is usually referred to as the *central* or *reference* unit cell.

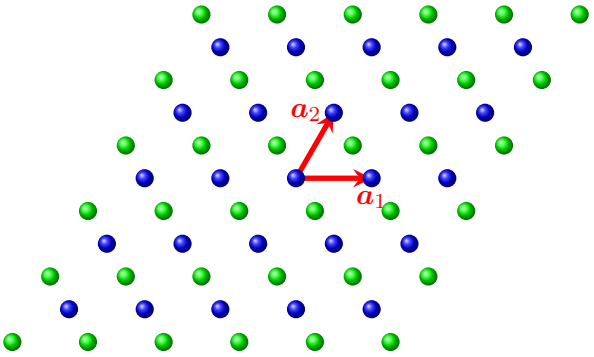

Figure 4.1. Two-dimensional hexagonal Bravais lattice with two atoms in a unit cell (blue and green).

4.1.2 Bloch theorem

An operator A is translationally invariant iff it commutes with all translation operators $t_{\boldsymbol{m}}$ for all lattice vectors $\boldsymbol{m}$:

$$\forall \boldsymbol{m} : [A, t_{\boldsymbol{m}}] = 0, \tag{4.2}$$

where $t_{\boldsymbol{m}}$ is defined by its application to a function f as

$$(t_{\boldsymbol{m}} f)(\boldsymbol{r}) \equiv f(\boldsymbol{r} + \boldsymbol{m}). \tag{4.3}$$

In the coordinate representation, operators depend on the electron coordinates $\boldsymbol{r}$, its momentum $\boldsymbol{p}$ and spin given by $\boldsymbol{\sigma}$. Since translations only affect the electron coordinates, the momentum operator $\boldsymbol{p}$, as well as the spin operator $\boldsymbol{\sigma}$ are translationally invariant, and the condition in Eq. (4.2) reduces to

$$\forall \boldsymbol{m} : A(\boldsymbol{r} + \boldsymbol{m}) = A(\boldsymbol{r}), \tag{4.4}$$

i.e. $A(\boldsymbol{r})$ must be a *periodic* function with the lattice periodicity. Note that the electron dipole moment $\mu \equiv -\boldsymbol{r}$ defining the external potential in Eq. (3.28) is not periodic.

A periodic system consists of atoms placed in unit cells that are periodically replicated. The electron–nuclear attraction potential

$$V(\boldsymbol{r}) = \sum_{\boldsymbol{m}A} \frac{-Z_A}{|\boldsymbol{r} - \boldsymbol{A} - \boldsymbol{m}|} \tag{4.5}$$

therefore satisfies Eq. (4.4). Here, A labels the atoms in a unit cell, and Z_A and $\boldsymbol{A}$ is their charge and position, respectively. This means that the one-electron Hamiltonian h commutes with all translation operators. The consequence of this translational symmetry is called the *Bloch theorem*,[105] which states:[64,106–108]

Theorem 3 (Bloch)**.** *Let $\psi(\boldsymbol{r})$ denote an eigenfunction of the translationally invariant one-electron Hamiltonian h, i.e. $\forall \boldsymbol{m} : [h, t_{\boldsymbol{m}}] = 0$ and $h\psi(\boldsymbol{r}) = \varepsilon\psi(\boldsymbol{r})$. Then $\psi(\boldsymbol{r})$ takes the form of*

$$\psi(\boldsymbol{r}) = e^{i\boldsymbol{k}\cdot\boldsymbol{r}} u(\boldsymbol{r}), \tag{4.6}$$

for some $\boldsymbol{k}$ and a periodic function u; $u(\boldsymbol{r} + \boldsymbol{m}) = u(\boldsymbol{r})$.

Proof. Within quantum theory, commuting operators have a common set of eigenfunctions. In case of the translational symmetry, each eigenfunction of the Hamiltonian is also an eigenfunction of all the translation operators $t_{\boldsymbol{m}}$ (there is no degeneracy). This is because the translational group is Abelian (commutative), and the irreducible representations of an Abelian group are one-dimensional (see Hamermesh[109]). Therefore, we can state that

$$t_{\boldsymbol{m}}\psi(\boldsymbol{r}) \equiv \psi(\boldsymbol{r}+\boldsymbol{m}) = \lambda_{\boldsymbol{m}}\psi(\boldsymbol{r}).$$

We require the electron density [Eq. (1.20)] to be periodic, so

$$\rho(\boldsymbol{r}+\boldsymbol{m}) \equiv \psi^\dagger(\boldsymbol{r}+\boldsymbol{m})\psi(\boldsymbol{r}+\boldsymbol{m}) = |\lambda_{\boldsymbol{m}}|^2\psi^\dagger(\boldsymbol{r})\psi(\boldsymbol{r}) = |\lambda_{\boldsymbol{m}}|^2\rho(\boldsymbol{r}) = \rho(\boldsymbol{r})$$

implies that $\lambda_{\boldsymbol{m}} = e^{i\eta_{\boldsymbol{m}}}$ for $\eta_{\boldsymbol{m}} \in \mathbb{R}$. To find the expression for $\eta_{\boldsymbol{m}}$, consider a linear combination of lattice vectors $\boldsymbol{m}+l\boldsymbol{n}$, where $l \in \mathbb{Z}$. Hence,

$$\begin{aligned} t_{\boldsymbol{m}+l\boldsymbol{n}}\psi(\boldsymbol{r}) &\overset{1.}{=} e^{i\eta_{\boldsymbol{m}+l\boldsymbol{n}}}\psi(\boldsymbol{r}) \\ &\overset{2.}{=} \psi(\boldsymbol{r}+\boldsymbol{m}+l\boldsymbol{n}) = e^{i\eta_{\boldsymbol{m}}}(e^{i\eta_{\boldsymbol{n}}})^l\psi(\boldsymbol{r}). \end{aligned}$$

I follows, that $\eta_{\boldsymbol{m}}$ must be a linear function of $\boldsymbol{m}$:

$$\eta_{\boldsymbol{m}+l\boldsymbol{n}} = \eta_{\boldsymbol{m}} + l\eta_{\boldsymbol{n}},$$

and hence $\eta_{\boldsymbol{m}} = \boldsymbol{k}\cdot\boldsymbol{m}$ is the most general parameterization. Therefore,

$$\psi(\boldsymbol{r}+\boldsymbol{m}) = e^{i\boldsymbol{k}\cdot\boldsymbol{m}}\psi(\boldsymbol{r}). \tag{4.7}$$

Proving Eq.(4.6) is straightforward: Let us define u as

$$u(\boldsymbol{r}) \equiv e^{-i\boldsymbol{k}\cdot\boldsymbol{r}}\psi(\boldsymbol{r}).$$

Clearly, $u(\boldsymbol{r}+\boldsymbol{m}) = u(\boldsymbol{r})$. It follows, that $\psi(\boldsymbol{r}) = e^{i\boldsymbol{k}\cdot\boldsymbol{r}}u(\boldsymbol{r})$. □

As a consequence of the Bloch theorem, we can write the eigenfunctions of h, here denoted as ψ_p, as

$$\boxed{\psi_p(\boldsymbol{k};\boldsymbol{r}) = e^{i\boldsymbol{k}\cdot\boldsymbol{r}}u_p(\boldsymbol{k};\boldsymbol{r})}, \tag{4.8}$$

where u_p are periodic functions with the lattice periodicity, p and $\boldsymbol{k}$ are two quantum numbers that label the common eigenfunctions of h and $t_{\boldsymbol{m}}$.

The Bloch functions $\psi_p(\boldsymbol{k};\boldsymbol{r})$ satisfy the time-independent Schrödinger (or Dirac) equation

$$\boxed{h\psi_p(\boldsymbol{k};\boldsymbol{r}) = \varepsilon_p(\boldsymbol{k})\psi_p(\boldsymbol{k};\boldsymbol{r})}, \tag{4.9}$$

where $\varepsilon_p(\boldsymbol{k})$ are called the *band energies*. The Bloch theorem is usually applied in the context of band-structure calculations from the HF or KS equations. However, the proof of the theorem that is presented here and in many textbooks[64,106,107] only holds for the one-electron Hamiltonian, *i.e.* without the terms that depend on the density matrix or the electron density. The proper proof of the Bloch theorem in the SCF framework must consider periodicity of these terms as well.[108]

4.1.3 Reciprocal space

The vector $\boldsymbol{k}$ that labels the Bloch functions and the band energies is called the *quasimomentum*, and belongs to the first Brillouin zone, labeled $\mathcal{K}$. The first Brillouin zone is the central unit cell of reciprocal space[2] composed of the inverse lattice vectors $\boldsymbol{K}$ that are defined using the primitive direct-space vectors as

$$e^{i\boldsymbol{K}\cdot\boldsymbol{m}} = 1. \tag{4.10}$$

The inverse lattice is a Bravais lattice with primitive vectors $\boldsymbol{b}_i$, so $\boldsymbol{K}$ can be written as

$$\boldsymbol{K} = K^i\boldsymbol{b}_i. \tag{4.11}$$

The primitive vectors $\boldsymbol{b}_i$ constitute a biorthogonal basis with respect to the vectors $\boldsymbol{a}_i$, hence

$$\boldsymbol{a}_i \cdot \boldsymbol{b}_j = 2\pi\delta_{ij}. \tag{4.12}$$

It follows that the lattice vectors $\boldsymbol{K}$ constructed from Eq. (4.11) automatically satisfy the requirement in Eq. (4.10). The inverse primitive vectors $\boldsymbol{b}_i$ in three dimensions are obtained from $\boldsymbol{a}_i$ as

$$\boldsymbol{b}_1 = 2\pi\frac{\boldsymbol{a}_2 \times \boldsymbol{a}_3}{\boldsymbol{a}_1 \cdot (\boldsymbol{a}_2 \times \boldsymbol{a}_3)}, \tag{4.13}$$

where applying cyclic permutations yield the expressions for the remaining two vectors $\boldsymbol{b}_2$ and $\boldsymbol{b}_3$.

[2] Also referred to as inverse space or $\boldsymbol{k}$-space.

4.2 Band structure theory

4.2.1 Density of states

Solid-state calculations of the ground electronic state typically involve reporting $\boldsymbol{k}$-dependent band energies $\varepsilon_p(\boldsymbol{k})$, in addition to the cohesive energies.[3] Since the one-particle states form a continuum, one can calculate the *energy* density of states (DOS) for three-dimensional periodic systems using the band energies as[4]

$$N(\varepsilon) = \frac{1}{(2\pi)^3} \sum_p \int_{\mathcal{K}} d^3\boldsymbol{k} \delta(\varepsilon - \varepsilon_p(\boldsymbol{k})). \tag{4.14}$$

The DOS function measures the number of states per unit energy, per unit volume, near the energy ε. Integrating $N(\varepsilon)$ over the entire energy range gives

$$\int N(\varepsilon) d\varepsilon = \frac{1}{(2\pi)^3} N_\mathrm{b} |\mathcal{K}| = \frac{N_\mathrm{b}}{\mathcal{V}}, \tag{4.15}$$

where $\mathcal{V}$ and $|\mathcal{K}| \equiv \frac{(2\pi)^3}{\mathcal{V}}$ are the direct- and reciprocal-space unit-cell volumes, respectively, and N_b is the total number of bands. N_b is finite for calculations that employ finite basis sets. In practical calculations, DOS can be evaluated on a uniform grid of $\boldsymbol{k}$-points. Using the substitution

$$\frac{1}{(2\pi)^3} \int_{\mathcal{K}} d^3\boldsymbol{k} \to \frac{1}{(2\pi)^3} \sum_{\boldsymbol{k}} \frac{|\mathcal{K}|}{\mathcal{N}} = \frac{1}{\mathcal{V}\mathcal{N}} \sum_{\boldsymbol{k}}, \tag{4.16}$$

where $\mathcal{N}$ is the total number of $\boldsymbol{k}$-points, we obtain

$$N(\varepsilon) = \frac{1}{\mathcal{V}\mathcal{N}} \sum_{p\boldsymbol{k}} \delta(\varepsilon - \varepsilon_{p\boldsymbol{k}}). \tag{4.17}$$

Determining the DOS has several advantages. Many properties, such as the heat capacity, can be evaluated as energy integrals of the DOS. Moreover, the existence of the band gap of the ground state of a solid can be recognized from the knowledge of its DOS; this is useful if the band energies are not available.

[3] The cohesive energy is a measure of energy required to break bonds in a crystal, and form separated neutral atoms in their ground electronic state at 0K temperature and at atmospheric pressure. [107]

[4] This expression can trivially be modified for one- and two-dimensional periodic systems.

4.2.2 Band structure diagrams

The band energies $\varepsilon_p(\boldsymbol{k})$ are commonly shown in diagrams which contain the $\boldsymbol{k}$-points on the x-axis, and the band energies for each band p as functions of $\boldsymbol{k}$ on the y-axis. For simplicity, for two- and three-dimensional systems a path consisting of lines connecting special high-symmetry $\boldsymbol{k}$-points in the first Brillouin zone is formed. The band structure diagram can be used to classify systems according to the size of their band gap between the occupied and vacant bands as metals (zero band gap), semiconductors (small band gap), or insulators (large band gap, *e.g.* > 4 eV).[107] Hence, insulators and semiconductors only contain fully occupied or vacant bands, whereas metals contain bands that are partially occupied.

As an example, let us consider a one-dimensional periodic system with a lattice constant a. Eq. (4.12) implies that the reciprocal lattice constant is $b = \frac{2\pi}{a}$, and the first Brillouin zone is

$$\mathcal{K} = \left\{ k \in \mathbb{R} \;\middle|\; -\frac{\pi}{a} \leq k \leq \frac{\pi}{a} \right\}. \tag{4.18}$$

Fig. 4.2 shows the band structure and the DOS of polyacetylene with al-

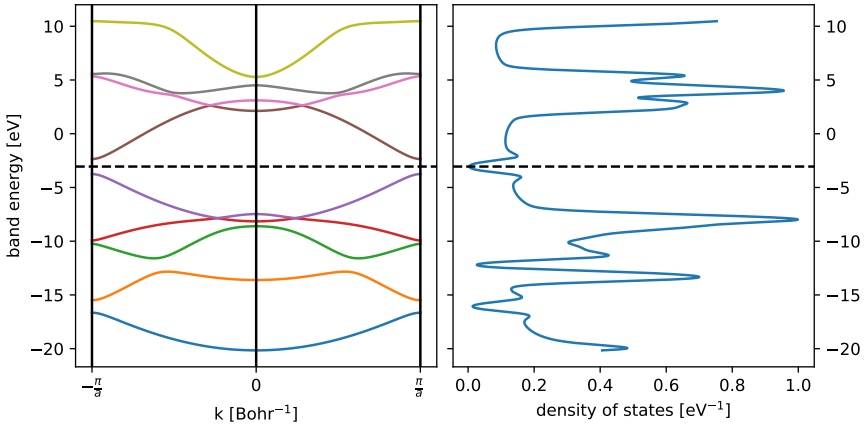

Figure 4.2. Band structure diagram (left) and DOS (right) of polyacetylene with alternating lengths of carbon–carbon bonds. The bands below the dashed line are fully occupied, and the bands above the dashed line are vacant, demonstrating that polyacetylene is a semiconductor with a nonzero band gap.

ternating lengths of carbon–carbon bonds that we have obtained from the solution of the periodic KS equation. We can see that the DOS is zero for the energies inside the band gap, classifying polyacetylene as a semiconductor.[110–112]

4.3 Periodic SCF equation

The formulation of the SCF equations for periodic systems employing the linear combination of atomic orbitals (LCAO) has been know for some time for the HF method[113,114] as well as for the DFT method.[115,116] Instead of using reciprocal space to express the Fock operator, its matrix elements are evaluated in real space.[117–120] Here, I briefly summarize this approach.[64,108]

The SCF equation for a periodic system is essentially the same as Eq. (2.39), *i.e.*

$$F\varphi_p(\boldsymbol{k};\boldsymbol{r}) = \varepsilon_p(\boldsymbol{k})\varphi_p(\boldsymbol{k};\boldsymbol{r}), \tag{4.19}$$

except that the solutions $\varphi_p(\boldsymbol{k};\boldsymbol{r})$ must satisfy the Bloch theorem

$$\varphi_p(\boldsymbol{k};\boldsymbol{r}+\boldsymbol{m}) = e^{i\boldsymbol{k}\cdot\boldsymbol{m}}\varphi_p(\boldsymbol{k};\boldsymbol{r}) \tag{4.20}$$

for each lattice vector $\boldsymbol{m}$ defined in Eq. (4.1). To ensure that this condition is fulfilled when an atom-centered basis is used, we construct a symmetry-adapted basis as

$$\chi_\mu(\boldsymbol{k};\boldsymbol{r}) = \frac{1}{\sqrt{|\mathcal{K}|}}\sum_{\boldsymbol{m}} e^{i\boldsymbol{k}\cdot\boldsymbol{m}}\chi_{\mu\boldsymbol{m}}(\boldsymbol{r}) \tag{4.21}$$

for $\boldsymbol{k} \in \mathcal{K}$. Here, $\chi_{\mu\boldsymbol{m}}(\boldsymbol{r})$ are the atom-centered basis functions of the periodic system, obtained for the unit cell $\boldsymbol{m}$ by translating the reference unit cell $\boldsymbol{m} = \boldsymbol{0}$ basis as

$$\chi_{\mu\boldsymbol{m}}(\boldsymbol{r}) \equiv \chi_\mu(\boldsymbol{r}-\boldsymbol{m}). \tag{4.22}$$

Eq. (4.19) written in this basis takes the form

$$\boxed{F(\boldsymbol{k})c(\boldsymbol{k}) = S(\boldsymbol{k})c(\boldsymbol{k})\varepsilon(\boldsymbol{k})}, \tag{4.23}$$

where $c(\boldsymbol{k})$ is the matrix of the expansion coefficients (for each $\boldsymbol{k}$-point),

$\varepsilon(\boldsymbol{k})$ is the diagonal matrix of band energies, and

$$F_{\mu\mu'}(\boldsymbol{k}) = \sum_{\boldsymbol{m}} e^{i\boldsymbol{k}\cdot\boldsymbol{m}} F_{\mu\boldsymbol{0},\mu'\boldsymbol{m}}, \tag{4.24a}$$

$$S_{\mu\mu'}(\boldsymbol{k}) = \sum_{\boldsymbol{m}} e^{i\boldsymbol{k}\cdot\boldsymbol{m}} S_{\mu\boldsymbol{0}.\mu'\boldsymbol{m}}, \tag{4.24b}$$

The real-space matrix elements are evaluated as

$$F_{\mu\boldsymbol{0},\mu'\boldsymbol{m}} = \int_{\mathbb{R}^3} \chi^{\dagger}_{\mu\boldsymbol{0}}(\boldsymbol{r}) F \chi_{\mu'\boldsymbol{m}}(\boldsymbol{r}) d^3\boldsymbol{r}, \tag{4.25a}$$

$$S_{\mu\boldsymbol{0},\mu'\boldsymbol{m}} = \int_{\mathbb{R}^3} \chi^{\dagger}_{\mu\boldsymbol{0}}(\boldsymbol{r}) \chi_{\mu'\boldsymbol{m}}(\boldsymbol{r}) d^3\boldsymbol{r}. \tag{4.25b}$$

The density matrix is constructed using the diagonal matrix of occupation numbers $f(\boldsymbol{k})$ as

$$D(\boldsymbol{k}) = c(\boldsymbol{k}) f(\boldsymbol{k}) c^{\dagger}(\boldsymbol{k}), \tag{4.26}$$

and transformed to real space by evaluating the reciprocal-space integral

$$D^{\mu\boldsymbol{m},\mu'\boldsymbol{0}} = \frac{1}{|\mathcal{K}|} \int_{\mathcal{K}} e^{i\boldsymbol{k}\cdot\boldsymbol{m}} D^{\mu\mu'}(\boldsymbol{k}) d^3\boldsymbol{k}. \tag{4.27}$$

We calculate this integral on a uniform grid of evenly distributed $\boldsymbol{k}$-points, however, for systems with the small or zero band gap, special techniques for the integration in $\boldsymbol{k}$-space must be invoked to capture possible oscillations of the density matrix in reciprocal space.[119,121–124]

4.4 Summary of contributions in Paper V

The relativistic SCF methodology of Chapters 1 and 2 is extended to the solid-state domain in **Paper V** in order to enable variational calculations of relativistic band structures of periodic systems. Our method is based on the atom-centered GTO basis functions defined in Section 2.5 that constitute the 4c basis in Eq. (1.30) so that the RKB condition[35] Eq. (1.27) is satisfied. All matrix elements of operators are expressed in real space, as in previous nonrelativistic approaches,[116,119,120,125] and transformed to reciprocal space for the diagonalization step of the SCF procedure. The real-space formulation of the 4c Fock matrix enables us to employ a very compact quaternion-based representation[47,51,126] (see also **Paper IV**) that exploits the time-reversal symmetry of the operators within the Kramers restricted framework.[47,49,51]

In **Paper V** we show that the reciprocal-space matrices expressed using the RKB atom-centered basis take the form of

$$A_{\mu\mu'}(\boldsymbol{k}) = \begin{pmatrix} a(\boldsymbol{k}) & b(\boldsymbol{k}) \\ -b^*(-\boldsymbol{k}) & a^*(-\boldsymbol{k}) \end{pmatrix}_{\mu\mu'}, \tag{4.28}$$

which is a generalization of the time-reversal-symmetric structure in Eq. (1.41) discussed in Section 1.4. This matrix structure requires using quaternions with complex-valued components, in contrast to Eq. (1.42), where the quaternion components were defined as real. If the SOC is not neglected in the 4c (or 2c) theory,[46] (see the discussion below Eq. (1.33)), then the reciprocal-space Fock matrix has the structure of Eq. (4.28) with $b(\boldsymbol{k}) \neq 0$ and $a(\boldsymbol{k}) \neq a^*(-\boldsymbol{k})$. The additional absence of space inversion symmetry in materials leads to the well-known spin splittings of bands.[127–131] In **Paper V** we prove that the time-reversal-symmetric structures in reciprocal and real spaces are preserved throughout the SCF procedure.

The electron density in Eq. (2.27) is adapted for periodic systems by exploiting the translational invariance of the density matrix. Therefore,

$$\rho(\boldsymbol{r}) = \sum_{\boldsymbol{mn}} \mathrm{Tr}\left[\Omega_{\mu\boldsymbol{0},\mu'\boldsymbol{m}}(\boldsymbol{r}-\boldsymbol{n}) D^{\mu'\boldsymbol{m},\mu\boldsymbol{0}}\right]. \tag{4.29}$$

To ensure the convergence of the electrostatic lattice sums of Coulomb interactions,[132] we construct the total *charge* density ρ^{ch} so that the unit cells are electrically neutral[133–135] as

$$\rho^{\mathrm{ch}}(\boldsymbol{r}) = \sum_{\boldsymbol{n}} \tilde{\rho}^{\mathrm{ch}}(\boldsymbol{r}-\boldsymbol{n}), \tag{4.30}$$

$$\tilde{\rho}^{\mathrm{ch}}(\boldsymbol{r}) = \sum_{A} Z_A \delta(\boldsymbol{r}-\boldsymbol{A}) - \sum_{\boldsymbol{m}} \mathrm{Tr}\left[\Omega_{\mu\boldsymbol{0},\mu'\boldsymbol{m}}(\boldsymbol{r}) D^{\mu'\boldsymbol{m},\mu\boldsymbol{0}}\right]. \tag{4.31}$$

We evaluate the real-space Coulomb matrix by employing the techniques based on the multipole expansion.[79,80] The infinite lattice sums of interaction tensors are computed using the iterative renormalization procedure,[136,137] proof of which we provide in the appendix of **V**. The problems associated with the conditional convergence of the three-dimensional lattice sums[132,138] are resolved by eliminating the unit cell dipole moment by introducing fictitious charges on the unit cell face centers.[134,139]

Finally, we assessed the method by calculating the total energies and the band gaps of the three-dimensional silver halides (AgX for X=Cl, Br,

I) in their face-centered cubic (FCC) structure. We report the band gaps evaluated at various special $\boldsymbol{k}$-points. The unit cell of AgX has a nonzero dipole moment, and thus these systems serve as a test of the validity of the computational scheme for the most general case of the lattice sums appearing in the Coulomb potential.

To examine the effect of the SOC, we calculated the relativistic and the nonrelativistic band structures of the two-dimensional graphene-like honeycomb systems (see Fig. 4.3), silicene and germanene, known to exhibit the quantum spin Hall effect.[28–31] Contrary to the graphene, its heavier counterparts are stable in a buckled structure which further enhances the SOC.[29] Fig. 4.4 shows the first Brillouin zone of the two-dimensional hexagonal lattice and the chosen path in reciprocal space used for the band structure diagram in Fig. 4.5. Fig. 4.6 depicts the surface plot of the highest occupied band and the lowest unoccupied band obtained at the relativistic level of theory. Two Dirac cones can be seen in the plot, as well as the nonzero (albeit very small) band gap between the bands at the Dirac points.[5]

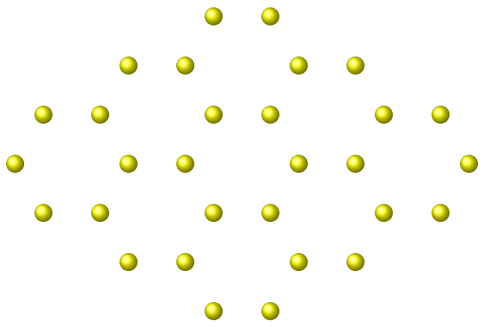

Figure 4.3. Two-dimensional honeycomb structure of silicene and germanene.

[5]The valence band and conduction band of some two-dimensional materials (such as topological insulators) take the shape of two conical surfaces (Dirac cones) that meet near the Fermi level at special $\boldsymbol{k}$-points called Dirac points. Due to this linear dispersion relation, these materials exhibit unusual transport properties and lead to various quantum Hall effects.[140]

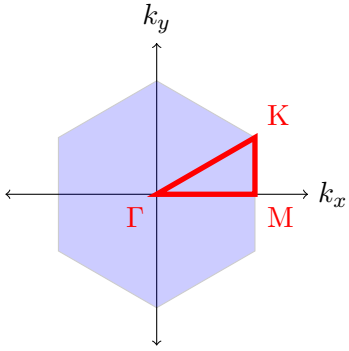

Figure 4.4. First Brillouin zone of the two-dimensional hexagonal lattice. The path Γ–M–K–Γ is conventionally chosen for band structure diagrams.

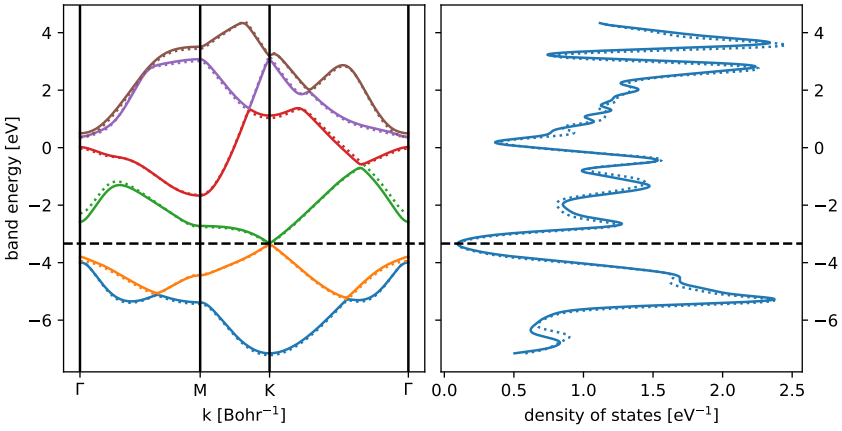

Figure 4.5. Band structure diagram (left) and the DOS (right) of the two-dimensional germanene. The full and dashed colored curves were obtained from the relativistic and nonrelativistic calculations, respectively. The black horizontal dashed line depicts the Fermi level. The Dirac cone is found in the K-point.

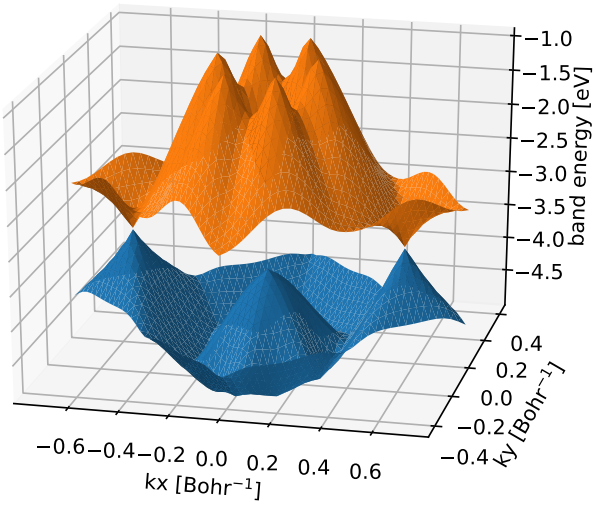

Figure 4.6. Two-dimensional band structure surface plot of the highest occupied band (blue) and the lowest unoccupied band (orange) of the two-dimensional germanene obtained from the relativistic calculation. The plot is constructed for the $\boldsymbol{k}$-points in the first Brillouin zone. The small band gap can be seen at the two distinct Dirac points.

Appendix A

Covariance and contravariance

Components of vectors (functions), matrices (operators), and higher-ranking tensors can transform in two distinct ways upon a change of basis. For example, consider F to be the Fock matrix expressed in some basis (*e.g.* AOs), and F' to be the Fock matrix expressed in some other basis (*e.g.* orthogonal AOs). Let L denote the transformation matrix between the two bases. Then

$$F' = L^\dagger F L, \qquad\qquad F = (L^\dagger)^{-1} F' L^{-1}. \tag{A.1}$$

On the other hand, the density matrices D and D' expressed in the corresponding bases satisfy

$$D' = L^{-1} D (L^\dagger)^{-1}, \qquad\qquad D = L^\dagger D' L. \tag{A.2}$$

These transformation relations ensure that the trace of the product of F and D remains invariant upon the change of basis, *i.e.*

$$\mathrm{Tr}\,(F'D') = \mathrm{Tr}\left(L^\dagger F L L^{-1} D (L^\dagger)^{-1}\right) = \mathrm{Tr}\,(FD)\,. \tag{A.3}$$

Therefore, it is a common habit in multilinear algebra and tensor analysis to distinguish between the two types of tensor components (called *covariant* and *contravariant*) by typesetting their respective indices as subscripts for covariant indices (*e.g.* $A_{\mu\nu}$), and superscripts for contravariant

indices (*e.g.* $A^{\mu\nu}$). Since covariant and contravariant components of a tensor are the same when expressed in an orthonormal basis, this distinction only becomes relevant when a non-orthonormal basis is considered.[1] Here I briefly summarize the main implications of the concept of covariance and contravariance to molecular quantum mechanics, while concentrating on the common conventions used in the field, rather than a systematic explanation of multilinear algebra. As a result of distinguishing between the two types of indices, the overlap matrix will appear naturally in all expressions encountered in this work.[2] Works of Head-Gordon *et al.*[73,74] contain more detailed information on the tensor formalism in quantum chemistry.

Let $\chi_\mu(\boldsymbol{r})$ denote a (possibly non-orthogonal) basis function. Any well-behaved function $f(\boldsymbol{r})$ can be expanded as

$$f(\boldsymbol{r}) = f^\mu \chi_\mu(\boldsymbol{r}), \tag{A.4}$$

where f^μ are the expansion coefficients. Since f^μ are vector components with respect to the basis χ_μ, they transform contravariantly, and are traditionally denoted with an *upper* index. The basis functions χ_μ transform covariantly, and are thus denoted with a *lower* index. The overlap matrix

$$S_{\mu\nu} = \int \chi_\mu^\dagger(\boldsymbol{r}) \chi_\nu(\boldsymbol{r}) d^3\boldsymbol{r} \tag{A.5}$$

plays a role of the *metric tensor*, and can be used to define covariant components f_μ as

$$f_\mu = S_{\mu\nu} f^\nu. \tag{A.6}$$

Similarly, the inverse of the metric tensor $S^{\mu\nu}$ (defined by the identity $S_{\mu\rho}S^{\rho\nu} = \delta_\mu^\nu$) can be used to obtain contravariant components f^μ from the covariant components f_μ as

$$f^\mu = S^{\mu\nu} f_\nu. \tag{A.7}$$

Using the metric tensor S it is easy to prove the following index identity

$$u_\mu v^\mu = u^\mu v_\mu \tag{A.8}$$

[1] To be precise, this is only true if a metric tensor is available to map each covariant component onto a contravariant component and vice versa.

[2] This section was written as a consequence of the author's own concern while answering a seemingly trivial question "Why do overlap matrices even appear in equations? Shouldn't equations in physics be invariant with respect to the basis that is used to express them?".

for any u, v; the identity can be generalized to hold for arbitrary tensors.

In molecular quantum mechanics, matrix elements of an operator A are naturally calculated using an integral over the basis functions χ_ν and $\chi_\mu^\dagger$ as

$$A_{\mu\nu} = \int \chi_\mu^\dagger(\boldsymbol{r}) A \chi_\nu(\boldsymbol{r}) d^3\boldsymbol{r}, \tag{A.9}$$

hence both indices $\mu\nu$ transform covariantly, contrary to matrix elements A^μ_ν, which would correspondent to an operator in the linear-algebraic sense. It is a common convention in quantum chemistry to imply that both indices of operators are covariant, even when they are sometimes omitted. Molecular orbitals $\varphi_i(\boldsymbol{r})$ are expanded according to Eq. (A.4) as

$$\varphi_p(\boldsymbol{r}) = \chi_\mu(\boldsymbol{r}) c^\mu{}_p, \tag{A.10}$$

where $c^\mu{}_p$ are the molecular orbital (MO) coefficients. The one-electron density matrix elements $D^{\mu\nu}$ transform contravariantly, so that expectation values $A_{\mu\nu}D^{\nu\mu}$ are invariant with respect to a change of basis. As a consequence of these conventions, the overlap matrix must appear in some expressions, *e.g.* a commutator of an operator F with the density matrix

$$[F, D]^\mu{}_\nu \equiv F^\mu{}_\rho D^\rho{}_\nu - D^\mu{}_\rho F^\rho{}_\nu \tag{A.11}$$

becomes

$$[F, D]_{\mu\nu} = F_{\mu\rho} D^{\rho\sigma} S_{\sigma\nu} - S_{\mu\rho} D^{\rho\sigma} F_{\sigma\nu}. \tag{A.12}$$

Theorem 4. *Let L be a transformation matrix between a complete (non-orthonormal) basis and an orthonormal basis, then*

$$L^\dagger S L = \mathbb{I}, \qquad\qquad L^{*\mu}{}_p S_{\mu\nu} L^\nu{}_q = \delta_{pq}. \tag{A.13}$$

Proof. The statement follows directly from the requirement that the metric tensor expressed in the orthonormal basis equals the identity matrix, *i.e.* $S_{pq} \equiv \delta_{pq}$. □

Bibliography

[1] A. Einstein, "Zur elektrodynamik bewegter körper," Ann. Phys. **17**, 891 (1905).

[2] L. Pauling, *The Nature of the Chemical Bond and the Structure of Molecules and Crystals: An Introduction to Modern Structural Chemistry* (Cornell university press, New York, 1960).

[3] E. Schrödinger, "An undulatory theory of the mechanics of atoms and molecules," Phys. Rev. **28**, 1049 (1926).

[4] P. A. Dirac, "The quantum theory of the electron," Proc. R. Soc. A **117**, 610 (1928).

[5] L. Pincherle, "Sull'intensità dello spettro di linee di raggi X del Tungsteno," Il Nuovo Cimento (1924-1942) **10**, 344 (1933).

[6] D. F. Mayers, "Relativistic self-consistent field calculation for mercury," Proc. R. Soc. A **241**, 93 (1957).

[7] N. E. Christensen and B. Seraphin, "Relativistic band calculation and the optical properties of gold," Phys. Rev. B **4**, 3321 (1971).

[8] J. Desclaux and P. Pyykkö, "Dirac-Fock one-centre calculations. The molecules CuH, AgH and AuH including p-type symmetry functions," Chem. Phys. Lett. **39**, 300 (1976).

[9] P. Schwerdtfeger, "Relativistic effects in properties of gold," Heteroat. Chem. **13**, 578 (2002).

[10] P. Pyykko and J. P. Desclaux, "Relativity and the periodic system of elements," Acc. Chem. Res. **12**, 276 (1979).

[11] L. J. Norrby, "Why is mercury liquid? Or, why do relativistic effects not get into chemistry textbooks?" J. Chem. Educ. **68**, 110 (1991).

[12] F. Calvo, E. Pahl, M. Wormit, and P. Schwerdtfeger, "Evidence for Low-Temperature Melting of Mercury owing to Relativity," Angew. Chem. Int. Ed. **52**, 7583 (2013).

[13] R. Ahuja, A. Blomqvist, P. Larsson, P. Pyykkö, and P. Zaleski-Ejgierd, "Relativity and the lead-acid battery," Phys. Rev. Lett. **106**, 018301 (2011).

[14] N. Christensen, S. Satpathy, and Z. Pawlowska, "First-principles theory of tetrahedral bonding and crystal structure of lead," Phys. Rev. B **34**, 5977 (1986).

[15] P. Pyykko, "Relativistic effects in structural chemistry," Chem. Rev. **88**, 563 (1988).

[16] T. Söhnel, H. Hermann, and P. Schwerdtfeger, "Towards the Understanding of Solid-State Structures: From Cubic to Chainlike Arrangements in Group 11 Halides," Angew. Chem. Int. Ed. **40**, 4381 (2001).

[17] A. Hermann, J. Furthmüller, H. W. Gäggeler, and P. Schwerdtfeger, "Spin-orbit effects in structural and electronic properties for the solid state of the group-14 elements from carbon to superheavy element 114," Phys. Rev. B **82**, 155116 (2010).

[18] N. Christensen and J. Kollar, "Electronic structure of CsAu," Solid State Commun. **46**, 727 (1983).

[19] C. L. Kane and E. J. Mele, "Quantum spin Hall effect in graphene," Phys. Rev. Lett. **95**, 226801 (2005).

[20] M. Z. Hasan and C. L. Kane, "Colloquium: topological insulators," Rev. Mod. Phys. **82**, 3045 (2010).

[21] L. Kou, Y. Ma, Z. Sun, T. Heine, and C. Chen, "Two-Dimensional Topological Insulators: Progress and Prospects," J. Phys. Chem. Lett. **8**, 1905 (2017).

[22] E. Rashba, "Theory of electrical spin injection: Tunnel contacts as a solution of the conductivity mismatch problem," Phys. Rev. B **62**, R16267 (2000).

[23] S. Wolf, D. Awschalom, R. Buhrman, J. Daughton, S. Von Molnar, M. Roukes, A. Y. Chtchelkanova, and D. Treger, "Spintronics: a spin-based electronics vision for the future," Science **294**, 1488 (2001).

[24] I. Žutić, J. Fabian, and S. D. Sarma, "Spintronics: Fundamentals and applications," Rev. Mod. Phys. **76**, 323 (2004).

[25] Z. Zhu, Y. Cheng, and U. Schwingenschlögl, "Giant spin-orbit-induced spin splitting in two-dimensional transition-metal dichalcogenide semiconductors," Phys. Rev. B **84**, 153402 (2011).

[26] T. Heine, "Transition metal chalcogenides: ultrathin inorganic materials with tunable electronic properties," Acc. Chem. Res. **48**, 65 (2014).

[27] X. Xu, W. Yao, D. Xiao, and T. F. Heinz, "Spin and pseudospins in layered transition metal dichalcogenides," Nat. Phys. **10**, 343 (2014).

[28] M. Gmitra, S. Konschuh, C. Ertler, C. Ambrosch-Draxl, and J. Fabian, "Band-structure topologies of graphene: Spin-orbit coupling effects from first principles," Phys. Rev. B **80**, 235431 (2009).

[29] C.-C. Liu, W. Feng, and Y. Yao, "Quantum spin Hall effect in silicene and two-dimensional germanium," Phys. Rev. Lett. **107**, 076802 (2011).

[30] Y. Xu, B. Yan, H.-J. Zhang, J. Wang, G. Xu, P. Tang, W. Duan, and S.-C. Zhang, "Large-gap quantum spin Hall insulators in tin films," Phys. Rev. Lett. **111**, 136804 (2013).

[31] W. Han, R. K. Kawakami, M. Gmitra, and J. Fabian, "Graphene spintronics," Nat. Nanotechnol. **9**, 794 (2014).

[32] ReSpect 5.0.1 (2018), *relativistic spectroscopy DFT program* of authors M. Repisky, S. Komorovsky, V. G. Malkin, O. L. Malkina,

M. Kaupp, K. Ruud, with contributions from R. Bast, R. Di Remigio, U. Ekstrom, M. Kadek, S. Knecht, L. Konecny, E. Malkin, I. Malkin Ondik (http://www.respectprogram.org/).

[33] InteRest (2018), *an integral library for relativistic quantum chemistry* of M. Repisky.

[34] XCFun (2010), *a library of DFT exchange-correlation functionals* of U. Ekström and contributors (https://github.com/dftlibs/xcfun).

[35] R. E. Stanton and S. Havriliak, "Kinetic balance: A partial solution to the problem of variational safety in Dirac calculations," J. Chem. Phys. **81**, 1910 (1984).

[36] R. McWeeny, *Methods of molecular quantum mechanics* (Academic Press, London, 1992).

[37] K. G. Dyall and K. Faegri, *Introduction to relativistic quantum chemistry* (Oxford University Press, New York, 2007).

[38] M. Reiher and A. Wolf, *Relativistic quantum chemistry: the fundamental theory of molecular science* (John Wiley & Sons, Weinheim, 2009).

[39] T. Saue, "Relativistic Hamiltonians for chemistry: a primer," ChemPhysChem **12**, 3077 (2011).

[40] F. Rosicky and F. Mark, "Approximate relativistic Hartree-Fock equations and their solution within a minimum basis set of slater-type functions," Theor. Chim. Acta **54**, 35 (1979).

[41] F. Mark, B. Lischka, and F. Rosicky, "Variational solution of the Dirac equation within a multicentre basis set of Gaussian functions," Chem. Phys. Lett. **71**, 507 (1980).

[42] Y. S. Lee and A. McLean, "Relativistic effects on R e and D e in AgH and AuH from all-electron Dirac–Hartree–Fock calculations," J. Chem. Phys. **76**, 735 (1982).

[43] I. P. Grant, "Conditions for convergence of variational solutions of Dirac's equation in a finite basis," Phys. Rev. A **25**, 1230 (1982).

[44] S. Komorovsky, M. Repisky, O. L. Malkina, V. G. Malkin, I. Malkin Ondik, and M. Kaupp, "A fully relativistic method for calculation of nuclear magnetic shielding tensors with a restricted magnetically balanced basis in the framework of the matrix Dirac–Kohn–Sham equation," J. Chem. Phys. **128**, 104101 (2008).

[45] W. Kutzelnigg, "Basis set expansion of the Dirac operator without variational collapse," Int. J. Quantum Chem. **25**, 107 (1984).

[46] K. G. Dyall, "An exact separation of the spin-free and spin-dependent terms of the Dirac–Coulomb–Breit Hamiltonian," J. Chem. Phys. **100**, 2118 (1994).

[47] T. Saue, Ph.D. thesis, University of Oslo (1996).

[48] S. Komorovsky, M. Repisky, and L. Bucinsky, "New quantum number for the many-electron Dirac-Coulomb Hamiltonian," Phys. Rev. A **94**, 052104 (2016).

[49] G. Aucar, H. A. Jensen, and J. Oddershede, "Operator representations in Kramers bases," Chem. Phys. Lett. **232**, 47 (1995).

[50] H. Jørgen Aa. Jensen, K. G. Dyall, T. Saue, and K. Fægri Jr, "Relativistic four-component multiconfigurational self-consistent-field theory for molecules: Formalism," J. Chem. Phys. **104**, 4083 (1996).

[51] T. Saue, K. Fægri, T. Helgaker, and O. Gropen, "Principles of direct 4-component relativistic SCF: application to caesium auride," Mol. Phys. **91**, 937 (1997).

[52] C. Chang, M. Pelissier, and P. Durand, "Regular two-component Pauli-like effective Hamiltonians in Dirac theory," Phys. Scr. **34**, 394 (1986).

[53] E. v. Lenthe, E.-J. Baerends, and J. G. Snijders, "Relativistic regular two-component Hamiltonians," J. Chem. Phys. **99**, 4597 (1993).

[54] E. van Lenthe, E.-J. Baerends, and J. G. Snijders, "Relativistic total energy using regular approximations," J. Chem. Phys. **101**, 9783 (1994).

[55] L. L. Foldy and S. A. Wouthuysen, "On the Dirac theory of spin 1/2 particles and its non-relativistic limit," Phys. Rev. **78**, 29 (1950).

[56] M. Iliaš, H. J. A. Jensen, V. Kellö, B. O. Roos, and M. Urban, "Theoretical study of PbO and the PbO anion," Chem. Phys. Lett. **408**, 210 (2005).

[57] W. Kutzelnigg and W. Liu, "Quasirelativistic theory equivalent to fully relativistic theory," J. Chem. Phys. **123**, 241102 (2005).

[58] M. Iliaš and T. Saue, "An infinite-order two-component relativistic Hamiltonian by a simple one-step transformation," J. Chem. Phys. **126**, 064102 (2007).

[59] G. Breit, "The effect of retardation on the interaction of two electrons," Phys. Rev. **34**, 553 (1929).

[60] K.-N. Huang, "Orbit–orbit interaction," J. Chem. Phys. **71**, 3830 (1979).

[61] T. Saue and T. Helgaker, "Four-component relativistic Kohn–Sham theory," J. Comput. Chem. **23**, 814 (2002).

[62] M. Born and R. Oppenheimer, "Zur quantentheorie der molekeln," Ann. Phys. **389**, 457 (1927).

[63] T. Helgaker, P. Jorgensen, and J. Olsen, *Molecular electronic-structure theory* (John Wiley & Sons, Chichester, 2000).

[64] L. Piela, *Ideas of quantum chemistry* (Elsevier, Amsterdam, 2007).

[65] P. Hohenberg and W. Kohn, "Inhomogeneous electron gas," Phys. Rev. **136**, B864 (1964).

[66] W. Kohn and L. J. Sham, "Self-consistent equations including exchange and correlation effects," Phys. Rev. **140**, A1133 (1965).

[67] A. Rajagopal and J. Callaway, "Inhomogeneous electron gas," Phys. Rev. B **7**, 1912 (1973).

[68] J. C. Slater, "A simplification of the hartree-fock method," Phys. Rev. **81**, 385 (1951).

[69] S. H. Vosko, L. Wilk, and M. Nusair, "Accurate spin-dependent electron liquid correlation energies for local spin density calculations: a critical analysis," Can. J. Phys. **58**, 1200 (1980).

[70] J. P. Perdew, K. Burke, and M. Ernzerhof, "Generalized gradient approximation made simple," Phys. Rev. Lett. **77**, 3865 (1996).

[71] A. D. Becke, "A new mixing of Hartree–Fock and local density-functional theories," J. Chem. Phys. **98**, 1372 (1993).

[72] J. P. Perdew and K. Schmidt, "Jacob's ladder of density functional approximations for the exchange-correlation energy," in *AIP Conf. Proc.*, Vol. 577 (AIP, 2001) pp. 1–20.

[73] M. Head-Gordon, P. E. Maslen, and C. A. White, "A tensor formulation of many-electron theory in a nonorthogonal single-particle basis," J. Chem. Phys. **108**, 616 (1998).

[74] M. Head-Gordon, M. Lee, P. Maslen, T. Van Voorhis, S. Gwaltney, *et al.*, "Tensors in electronic structure theory: basic concepts and applications to electron correlation models," in *Modern Methods and Algorithms of Quantum Chemistry*, NIC series, Vol. 3, edited by J. Grotendorst (Citeseer, Jülich, 2000) pp. 593–638.

[75] P. Pulay, "Convergence acceleration of iterative sequences. The case of SCF iteration," Chem. Phys. Lett. **73**, 393 (1980).

[76] P. Pulay, "Improved SCF convergence acceleration," J. Comput. Chem. **3**, 556 (1982).

[77] S. F. Boys, "Electronic wave functions-I. A general method of calculation for the stationary states of any molecular system," Proc. R. Soc. A **200**, 542 (1950).

[78] S. Obara and A. Saika, "Efficient recursive computation of molecular integrals over Cartesian Gaussian functions," J. Chem. Phys. **84**, 3963 (1986).

[79] C. A. White, B. G. Johnson, P. M. Gill, and M. Head-Gordon, "The continuous fast multipole method," Chem. Phys. Lett. **230**, 8 (1994).

[80] M. A. Watson, P. Sałek, P. Macak, and T. Helgaker, "Linear-scaling formation of Kohn-Sham Hamiltonian: Application to the calculation of excitation energies and polarizabilities of large molecular systems," J. Chem. Phys. **121**, 2915 (2004).

[81] J. Olsen and P. Jørgensen, "Linear and nonlinear response functions for an exact state and for an MCSCF state," J. Chem. Phys. **82**, 3235 (1985).

[82] K. Sasagane, F. Aiga, and R. Itoh, "Higher-order response theory based on the quasienergy derivatives: The derivation of the frequency-dependent polarizabilities and hyperpolarizabilities," J. Chem. Phys. **99**, 3738 (1993).

[83] A. J. Thorvaldsen, K. Ruud, K. Kristensen, P. Jørgensen, and S. Coriani, "A density matrix-based quasienergy formulation of the Kohn–Sham density functional response theory using perturbation-and time-dependent basis sets," J. Chem. Phys. **129**, 214108 (2008).

[84] J. Kauczor, P. Jørgensen, and P. Norman, "On the efficiency of algorithms for solving Hartree–Fock and Kohn–Sham response equations," J. Chem. Theory Comput. **7**, 1610 (2011).

[85] Helgaker, Trygve and Coriani, Sonia and Jørgensen, Poul and Kristensen, Kasper and Olsen, Jeppe and Ruud, Kenneth, "Recent advances in wave function-based methods of molecular-property calculations," Chem. Rev. **112**, 543 (2012).

[86] P. Norman, K. Ruud, and T. Saue, *Principles and Practices of Molecular Properties: Theory, Modeling, and Simulations* (John Wiley & Sons, Chichester, 2018).

[87] A. Dreuw and M. Head-Gordon, "Single-reference ab initio methods for the calculation of excited states of large molecules," Chem. Rev. **105**, 4009 (2005).

[88] D. J. Tannor, *Introduction to quantum mechanics* (University Science Books, Sausalito, California, 2007).

[89] L. Konecny, Ph.D. thesis, Comenius University (2017).

[90] M. Kadek, M.S. thesis, Comenius University (2013).

[91] E. Runge and E. K. Gross, "Density-functional theory for time-dependent systems," Phys. Rev. Lett. **52**, 997 (1984).

[92] R. van Leeuwen, "Mapping from densities to potentials in time-dependent density-functional theory," Phys. Rev. Lett. **82**, 3863 (1999).

[93] R. Kosloff, "Time-dependent quantum-mechanical methods for molecular dynamics," J. Phys. Chem. **92**, 2087 (1988).

[94] M. Hochbruck and C. Lubich, "On Magnus integrators for time-dependent Schrödinger equations," SIAM J. Numer. Anal. **41**, 945 (2003).

[95] A. Castro, M. A. Marques, and A. Rubio, "Propagators for the time-dependent Kohn–Sham equations," J. Chem. Phys. **121**, 3425 (2004).

[96] J. Jakowski and K. Morokuma, "Liouville–von Neumann molecular dynamics," J. Chem. Phys. **130**, 224106 (2009).

[97] J. Liu, Z. Guo, J. Sun, and W. Liang, "Theoretical studies on electronic spectroscopy and dynamics with the real-time time-dependent density functional theory," Front. Chem. China **5**, 11 (2010).

[98] K. Lopata and N. Govind, "Modeling fast electron dynamics with real-time time-dependent density functional theory: application to small molecules and chromophores," J. Chem. Theory Comput. **7**, 1344 (2011).

[99] W. Magnus, "On the exponential solution of differential equations for a linear operator," Commun. Pure Appl. Math. **7**, 649 (1954).

[100] U. Ekström, L. Visscher, R. Bast, A. J. Thorvaldsen, and K. Ruud, "Arbitrary-order density functional response theory from automatic differentiation," J. Chem. Theory Comput. **6**, 1971 (2010).

[101] J. J. Goings, P. J. Lestrange, and X. Li, "Real-time time-dependent electronic structure theory," Wiley Interdiscip. Rev. Comput. Mol. Sci. **8**, e1341 (2018).

[102] A. Bruner, D. LaMaster, and K. Lopata, "Accelerated broadband spectra using transition dipole decomposition and Padé approximants," J. Chem. Theory Comput. **12**, 3741 (2016).

[103] P. Fulde, *Electron correlations in molecules and solids*, Solid-State Sciences, Vol. 100 (Springer, Berlin, 1993).

[104] K. Lejaeghere, G. Bihlmayer, T. Björkman, P. Blaha, S. Blügel, V. Blum, D. Caliste, I. E. Castelli, S. J. Clark, A. Dal Corso, *et al.*, "Reproducibility in density functional theory calculations of solids," Science **351**, aad3000 (2016).

[105] F. Bloch, "Über die quantenmechanik der elektronen in kristallgittern," Z. Phys. **52**, 555 (1929).

[106] N. W. Ashcroft and N. D. Mermin, *Solid state physics* (Harcourt, Orlando, 1976).

[107] C. Kittel, *Introduction to solid state physics* (John Wiley & Sons, New York, 1996).

[108] C. Pisani, *Quantum-mechanical ab-initio calculation of the properties of crystalline materials* (Springer Science & Business Media, Berlin, 1996).

[109] M. Hamermesh, *Group theory and its application to physical problems* (Dover Publications, Inc., New York, 1989).

[110] A. Karpfen and R. Höller, "Cis-trans isomerism in infinite polyacetylenes: an ab initio study," Solid State Commun. **37**, 179 (1981).

[111] J. Brédas, R. Chance, R. Silbey, G. Nicolas, and P. Durand, "A nonempirical effective Hamiltonian technique for polymers: Application to polyacetylene and polydiacetylene," J. Chem. Phys. **75**, 255 (1981).

[112] S. Suhai, "Quasiparticle energy-band structures in semiconducting polymers: correlation effects on the band gap in polyacetylene," Phys. Rev. B **27**, 3506 (1983).

[113] J.-M. André, L. Gouverneur, and E. G. Leroy, "L'Etude Théorique des Systèmes Périodiques. I. La Méthode LCAO–HCO," Int. J. Quantum Chem. **1**, 427 (1967).

[114] J. M. André, "Self-Consistent Field Theory for the Electronic Structure of Polymers," J. Chem. Phys. **50**, 1536 (1969).

[115] M. Causa, R. Dovesi, C. Pisani, R. Colle, and A. Fortunelli, "Correlation correction to the Hartree-Fock total energy of solids," Phys. Rev. B **36**, 891 (1987).

[116] M. D. Towler, A. Zupan, and M. Causà, "Density functional theory in periodic systems using local Gaussian basis sets," Comput. Phys. Commun. **98**, 181 (1996).

[117] R. Euwema, D. Wilhite, and G. Surratt, "General crystalline hartree-fock formalism: Diamond results," Phys. Rev. B **7**, 818 (1973).

[118] R. Euwema, G. Wepfer, G. Surratt, and D. Wilhite, "Hartree-Fock calculations for crystalline Ne and LiF," Phys. Rev. B **9**, 5249 (1974).

[119] C. Pisani and R. Dovesi, "Exact-exchange Hartree–Fock calculations for periodic systems. I. Illustration of the method," Int. J. Quantum Chem. **17**, 501 (1980).

[120] R. Dovesi, C. Pisani, C. Roetti, and V. Saunders, "Treatment of Coulomb interactions in Hartree-Fock calculations of periodic systems," Phys. Rev. B **28**, 5781 (1983).

[121] G. Lehmann and M. Taut, "On the numerical calculation of the density of states and related properties," Phys. Status Solidi B **54**, 469 (1972).

[122] H. J. Monkhorst and J. D. Pack, "Special points for Brillouin-zone integrations," Phys. Rev. B **13**, 5188 (1976).

[123] G. Wiesenekker and E. Baerends, "Quadratic integration over the three-dimensional Brillouin zone," J. Phys. Condens. Matter **3**, 6721 (1991).

[124] P. E. Blöchl, O. Jepsen, and O. K. Andersen, "Improved tetrahedron method for Brillouin-zone integrations," Phys. Rev. B **49**, 16223 (1994).

[125] R. Łazarski, A. M. Burow, and M. Sierka, "Density functional theory for molecular and periodic systems using density fitting and continuous fast multipole methods," J. Chem. Theory Comput. **11**, 3029 (2015).

[126] M. Repisky, S. Komorovsky, and K. Ruud, (in preparation).

[127] G. Dresselhaus, "Spin-orbit coupling effects in zinc blende structures," Phys. Rev. **100**, 580 (1955).

[128] F. J. Ohkawa and Y. Uemura, "Quantized surface states of a narrow-gap semiconductor," J. Phys. Soc. Jpn. **37**, 1325 (1974).

[129] D. Broido and L. Sham, "Effective masses of holes at GaAs-AlGaAs heterojunctions," Phys. Rev. B **31**, 888 (1985).

[130] E. Rashba and E. Y. Sherman, "Spin-orbital band splitting in symmetric quantum wells," Phys. Lett. A **129**, 175 (1988).

[131] M. Cardona, N. Christensen, and G. Fasol, "Relativistic band structure and spin-orbit splitting of zinc-blende-type semiconductors," Phys. Rev. B **38**, 1806 (1988).

[132] S. W. de Leeuw, J. W. Perram, and E. R. Smith, "Simulation of electrostatic systems in periodic boundary conditions. I. Lattice sums and dielectric constants," Proc. R. Soc. A **373**, 27 (1980).

[133] J. Delhalle, L. Piela, J.-L. Brédas, and J.-M. André, "Multipole expansion in tight-binding Hartree-Fock calculations for infinite model polymers," Phys. Rev. B **22**, 6254 (1980).

[134] L. Z. Stolarczyk and L. Piela, "Direct calculation of lattice sums. A method to account for the crystal field effects," Int. J. Quantum Chem. **22**, 911 (1982).

[135] Y. Ohnishi and S. Hirata, "Charge-consistent redefinition of Fock integrals," Chem. Phys. **401**, 152 (2012).

[136] C. L. Berman and L. Greengard, "A renormalization method for the evaluation of lattice sums," J. Math. Phys. **35**, 6036 (1994).

[137] K. N. Kudin and G. E. Scuseria, "Revisiting infinite lattice sums with the periodic fast multipole method," J. Chem. Phys. **121**, 2886 (2004).

[138] L. Piela and L. Z. Stolarczyk, "On the relativity of short-and long-range effects in calculations for periodic systems," Chem. Phys. Lett. **86**, 195 (1982).

[139] K. N. Kudin and G. E. Scuseria, "A fast multipole method for periodic systems with arbitrary unit cell geometries," Chem. Phys. Lett. **283**, 61 (1998).

[140] B. A. Bernevig and T. L. Hughes, *Topological insulators and topological superconductors* (Princeton university press, Princeton, 2013).

Paper I

Excitation Energies from Real-Time Propagation of the Four-Component Dirac–Kohn–Sham Equation

M. Repisky, L. Konecny, M. Kadek, S. Komorovsky,
O. L. Malkin, V. G. Malkin and K. Ruud
J. Chem. Theory Comput. **11** (2015), 980–991.

Paper II

X-ray absorption resonances near $L_{2,3}$-edges from real-time propagation of the Dirac–Kohn–Sham density matrix

M. Kadek, L. Konecny, G. Bin, M. Repisky and K. Ruud
Phys. Chem. Chem. Phys. **17** (2015), 22566–22570.

Paper III

Acceleration of Relativistic Electron Dynamics by Means of X2C Transformation: Application to the Calculation of Nonlinear Optical Properties

L. Konecny, M. Kadek, S. Komorovsky,
O. L. Malkina, K. Ruud and M. Repisky
J. Chem. Theory Comput. **12** (2016), 5823–5833.

Paper IV

Resolution-of-identity accelerated relativistic two- and four-component electron dynamics approach to chiroptical spectroscopies

L. Konecny, M. Kadek, S. Komorovsky,
K. Ruud and M. Repisky
submitted to *J. Chem. Theory Comput.*

Paper V

All-electron fully relativistic Kohn–Sham theory for solids based on the Dirac–Coulomb Hamiltonian and Gaussian-type functions

M. Kadek, M. Repisky and K. Ruud
(in preparation)